Probabilistic Engineering Mechanics 80 (2025) 103776

Contents lists available at ScienceDirect

Probabilistic Engineering Mechanics

journal homepage: www.elsevier.com/locate/probengmech

Time-dependent uncertainty quantification analysis of complex dynamical systems☆

M. Ebadollahi[1], S. Rahman[*,2]

Department of Mechanical Engineering, The University of Iowa, Iowa City, IA 52242, USA

ARTICLE INFO

Keywords:
NARX
Dimensional decomposition
Orthogonal polynomials
Polynomial chaos expansion
Polynomial dimensional decomposition
Vehicle dynamics

ABSTRACT

This paper introduces a novel computational methodology, supported by robust numerical algorithms, for performing time-dependent uncertainty quantification (UQ) analysis on complex dynamical systems. The proposed approach consists of three key components: (1) a new stochastic adaptation of the nonlinear autoregressive with exogenous input (NARX) model, utilizing dimension-wise tensor product expansion to effectively capture the behavior of dynamical systems, (2) a polynomial dimensional decomposition (PDD) technique to propagate uncertainty in input random variables to the NARX coefficients, and (3) a unique integration between NARX and PDD, resulting in the PDD-NARX approximation for time-dependent UQ analysis. The PDD-NARX method distinguishes itself from conventional deterministic system identification tools by considering uncertainties originating from both the system's dynamic properties (e.g., mass, stiffness, and damping) and external forces (e.g., amplitude and frequency content of excitation time series). Unlike traditional methods, which rely on an intuitive selection of NARX basis functions, this approach employs dimensional decomposition and importance factors to systematically construct the NARX model function. Furthermore, PDD, due to its hierarchical, dimension-wise expansion, is better equipped to handle high-dimensional UQ problems than many existing methods, including the widely recognized polynomial chaos expansion. Numerical results demonstrate that low-order PDD-NARX approximations provide accurate and computationally efficient estimates of the probabilistic characteristics of simple dynamical systems. Moreover, the probabilistic vehicle dynamic analysis of a pick-up truck traversing road bumps underscores the effectiveness of the PDD-NARX method in addressing industrial-scale complex problems.

1. Introduction

Mathematical modeling and simulation of complex dynamical systems, whether natural or man-made, frequently require uncertainty quantification (UQ) analysis due to the inherent randomness in system properties, external excitations, and initial/boundary conditions [1–3]. The propagation of uncertainties from the input to the output of a dynamic system is typically assessed using sampling-based methods, such as crude Monte Carlo simulation (MCS). While MCS encompasses a broad class of computational algorithms that rely on repeated random sampling and is generally robust, it is often impractical, if not prohibitively expensive, when each instance of a full-scale dynamic analysis is computationally demanding.

Alternatively, several UQ methods or approximations exist, including polynomial chaos expansion (PCE) [4–6], polynomial dimensional decomposition (PDD) [7,8], stochastic collocation [9,10], and sparse-grid quadrature [11,12]. These methods are often used as surrogates for the computationally expensive MCS. While successful in conducting time-independent or quasi-static UQ analyses, these surrogate methods face significant challenges when applied to time-dependent or stochastic-dynamics problems [13–15]. In the absence of appropriate adaptations, the accuracy and efficiency of these methods degrade rapidly over time, often necessitating impractically high-order expansions or approximations to maintain desired accuracy and effectively capture the system dynamics. As a result, the fidelity and convergence properties of these surrogate methods may deteriorate substantially.

In 2010, Gerritsma et al. [13] introduced a time-dependent version of PCE to enhance the accuracy of long-time integration required for solving time-dependent UQ problems. The core idea of this adaptation involves using optimal orthogonal polynomials to construct the PCE at

☆ Grant sponsors: U.S. Department of Education, United States (Grant No. P116S210005); U.S. National Science Foundation (Grant No. CMMI-2317172).
* Corresponding author.
E-mail addresses: amin-ebadollahi@uiowa.edu (M. Ebadollahi), sharif-rahman@uiowa.edu (S. Rahman).
[1] Graduate Student.
[2] Professor.

https://doi.org/10.1016/j.probengmech.2025.103776
Received 10 March 2025; Received in revised form 30 April 2025; Accepted 8 May 2025
Available online 27 May 2025

discrete time instants, thereby recovering faster convergence properties for stochastic solutions over a defined time period. While this adaptation modestly improves the performance of standard PCE in solving elementary time-dependent problems, the fundamental challenge of long-time integration remains unresolved, particularly when dealing with large-scale, complex stochastic-dynamics problems.

For time-dependent problems of a more practical nature, system identification methods, such as the nonlinear autoregressive with exogenous input (NARX) model, provide an alternative approach to approximating dynamic system behavior. The NARX models achieve this by fitting selected input–output data pairs, whether simulated or measured, at and before the time instant of interest [16]. Although originally conceived as deterministic tools within the system identification community, stochastic extensions of NARX models are emerging, wherein a polynomial basis is typically employed to describe the model, with its parameters treated as random variables. For example, a PCE-NARX approximation, which combines PCE and NARX, has been used for UQ analysis of time-dependent problems [17,18]. While PCE-NARX represents a significant improvement over time-frozen PCE, two major challenges persist.

First, the selection of an appropriate basis for the NARX model remains largely intuitive and can be ambiguous, as multiple options exist. An improper choice of basis may lead to inaccurate predictions of the dynamic response, particularly if the nonlinearity with respect to the data pairs is not captured accurately. More critically, when the number of input–output data pairs is large, the tensor-product structure of the multivariate approximation results in an excessive number of basis functions, making the construction of the NARX model impractical. Therefore, identifying basis functions with superior approximation qualities in a systematic and efficient manner is essential for developing a stochastic NARX model with the fewest possible basis functions.

Second, since the coefficients of the stochastic NARX model are random, they must be statistically characterized by propagating the uncertainty in the input random variables that describe dynamic system properties (e.g., mass, stiffness, damping), external forces (e.g., amplitude, frequency), and initial/boundary conditions. In this context, Mai et al. [18] utilized PCE for uncertainty propagation in conjunction with NARX. However, alternative surrogate methods that may be better suited than PCE can also be integrated with NARX. The need for exploring alternatives arises from the fact that, in high-dimensional UQ problems commonly encountered in industrial-scale applications, the number of basis functions or expansion coefficients in PCE grows exponentially, thus succumbing to the curse of dimensionality. Consequently, there is a need for a strategic coupling between NARX and a more suitable surrogate method capable of deflating the curse of dimensionality. Such an approach would allow for solving a broader class of time-dependent UQ problems, including complex stochastic-dynamics problems, in a more efficient and computationally feasible manner.

The primary objective of this study is to introduce a novel computational method, referred to as the PDD-NARX approximation, along with its associated numerical algorithms, for time-dependent UQ analysis of complex dynamical systems. Section 2 presents the definition and setup of the time-dependent UQ problem, along with the necessary assumptions. In Section 3, the stochastic adaptation of the NARX model is described, utilizing dimensional decomposition followed by basis reduction via a four-step algorithm. This section also covers the estimation of NARX coefficients through regression. Section 4 introduces the analysis-of-variance (ANOVA) decomposition of the random NARX coefficients, leading to their PDD approximation. The process of calculating PDD coefficients from regression analysis is also detailed. In Section 5, the integration between PDD and NARX is explained, establishing the PDD-NARX approximation and its implementation. Section 6 presents two numerical examples: the first focuses on the convergence analysis of a stochastic ordinary differential equation (ODE), while the second involves a stochastic dynamic analysis of a two-degree-of-freedom (2DOF) car model. Section 7 addresses a large-scale engineering problem, where the probabilistic vehicle dynamic analysis of a pick-up truck is conducted, demonstrating the practical applicability of the PDD-NARX method developed in this study. Section 8 describes the future work. Section 9 provides conclusions drawn from the study.

2. UQ problem setup

Let $\mathbb{N} := \{1, 2, \ldots\}$, $\mathbb{N}_0 := \mathbb{N} \cup \{0\}$, $\mathbb{R} := (-\infty, +\infty)$, $\mathbb{R}_0^+ := [0, +\infty)$, and $\mathbb{R}^+ := (0, +\infty)$ be the sets of positive integers (natural), non-negative integers, all real numbers, non-negative real numbers, and positive real numbers, respectively. Denote by $\mathbb{A} := (a_k, b_k)$ an open or closed interval, where $a_k, b_k \in \mathbb{R}$ and $b_k > a_k$. Then, given $N \in \mathbb{N}$, $\mathbb{A}^N = \times_{k=1}^N (a_k, b_k)$ represents an open or closed bounded domain of $\mathbb{R}^N$.

2.1. Input random variables

Let $(\Omega, \mathcal{F}, \mathbb{P})$ be a probability space, where Ω is a sample space, $\mathcal{F}$ is a σ-field on Ω, and $\mathbb{P} : \mathcal{F} \to [0, 1]$ is a probability measure. With $\mathcal{B}^N$ representing the Borel σ-field on $\mathbb{A}^N$, $N \in \mathbb{N} := \{1, 2, \ldots\}$, consider an $\mathbb{R}^N$-valued continuous random vector $\mathbf{X} := \{X_1, \ldots, X_N\}^\intercal : (\Omega, \mathcal{F}) \to (\mathbb{A}^N, \mathcal{B}^N)$, which describes the statistical uncertainties in all input parameters of a stochastic-dynamics or time-dependent UQ problem. For instance, $\mathbf{X}$ may represent the amplitude and frequency content of the excitation time series; the dynamic system properties, such as mass, stiffness, and damping; and initial/boundary conditions. If some of these parameters are modeled as random fields or random processes, then $\mathbf{X}$ includes random variables due to their finite-dimensional discretizations. Denote by $f_{\mathbf{X}}(\mathbf{x})$ the joint probability density function (PDF) of $\mathbf{X}$. The ith component of $\mathbf{X}$ is a random variable X_i, which has the marginal PDF $f_{X_i}(x_i)$. The positive integer N, which represents the total number of input random variables, is often referred to as the dimension of the stochastic or UQ problem.

The requisite assumptions on input random variables are as follows.

Assumption 1. The input random vector $\mathbf{X} := \{X_1, \ldots, X_N\}^\intercal$ satisfies all of the following conditions:

1. All component random variables X_i, $i = 1, \ldots, N$, are statistically independent, but they are not necessarily identically distributed.
2. Each input random variable X_i, defined on a bounded or unbounded interval $\mathbb{A} := (a_k, b_k)$ of $\mathbb{R}$, has finite moments of all orders.
3. Each input random variable X_i has continuous marginal PDF $f_{X_i}(x_i)$ with a bounded or unbounded support $\mathbb{A}$. Moreover, given an infinite sequence of moments of X_i, the PDF $f_{X_i}(x_i)$ is uniquely determined.

Assumption 1 is frequently adopted by the UQ community.

2.2. Time-dependent UQ problem

Let $\mathbf{y}(t; \mathbf{X}) : [0, T] \times \mathbb{A}^N \to \mathbb{R}^K$, $T \in \mathbb{R}^+$, $K \in \mathbb{N}$, be a general K-dimensional vector-valued stochastic dynamic response of interest at time $t \in [0, T]$ and $L^2(\Omega, \mathcal{F}, P)$ a Hilbert space of square-integrable functions $\mathbf{y}$ with respect to $f_{\mathbf{X}}(\mathbf{x})d\mathbf{x}$. The arguments of the output function $\mathbf{y}$ indicate that it depends not only on time t, but also on the input random vector $\mathbf{X}$. For a general time-dependent UQ problem, $\mathbf{y}(t; \mathbf{X})$ satisfies P-almost surely the parameterized stochastic differential equations (SDEs)

$$\begin{aligned} \mathcal{A}\left[\mathbf{y}(t; \mathbf{X})\right] &= g(t; \mathbf{X}), \quad t \in [0, T] \subseteq \mathbb{R}_0^+, \, \mathbf{y} \in L^2(\Omega, \mathcal{F}, P), \\ C\left[\mathbf{y}(0; \mathbf{X})\right] &= q(\mathbf{X}), \end{aligned} \tag{1}$$

where $\mathcal{A}$ is a linear or nonlinear differential operator describing dynamics of discrete systems, C is an initial condition operator, and g and q, possibly random, are the forcing term and initial condition,

respectively. From the solution of Eq. (1), let $y(t;\mathbf{X})$ define any scalar-valued stochastic response component of $\mathbf{y}(t;\mathbf{X})$, where for notational simplicity the index of the component has been dropped. Associated with Eq. (1), a list, which is far from exhaustive, describes the following statistical and probabilistic solutions of a time-dependent UQ problem:

1. Calculate the second-moment properties of $y(t;\mathbf{X})$, that is, the mean $\mathbb{E}[y(t;\mathbf{X})]$ and variance $\mathbb{E}[y(t;\mathbf{X}) - \mathbb{E}[y(t;\mathbf{X})]]^2$; also, calculate higher-order moments of $y(t;\mathbf{X})$ if they exist.
2. Evaluate the PDF of $y(t;\mathbf{X})$.
3. Perform local sensitivity analysis of moments or PDF of $y(t;\mathbf{X})$ with respect to design variables $\mathbf{d}$, which may comprise distributional or structural parameters.
4. Calculate global sensitivities of $y(t;\mathbf{X})$ for a subset $\mathbf{X}_u$, $\emptyset \neq u \subset \{1,\dots,N\}$, of input variables. Both variance-based and density-based global sensitivity analyses are envisioned.
5. Conduct reliability analysis, e.g., compute the failure probability $P[\mathbf{X} \in \Omega_F(t)]$, which can be component-based analysis when $\Omega_F(t) := \{\mathbf{x} : y(t;\mathbf{x}) < y_0\}$ is defined by a single response function with y_0 representing a critical value or system-based analysis entailing multiple such functions.
6. Solve stochastic design optimization problems, that is, find $\mathbf{d}^* = \arg\min_{\mathbf{d}\in\mathbb{D}} c_0(\mathbf{d})$ for some cost function c_0 subject to a set of constraints $c_l(\mathbf{d}; y_l(t;\mathbf{x})) \leq c_{l,0}$, $l = 1,\dots,K, K \in \mathbb{N}$. Here, c_l depends on the lth dynamic response function $y_l(t;\mathbf{x})$ such that $\mathbf{y}$ satisfies Eq. (1).

A wide variety of SDEs, depending on the choice of operators and functions in Eq. (1) or similar equations, can be envisioned. Prominent among them are the stochastic initial-value problems from discrete dynamical systems, which are fundamental to various disciplines, including civil, aerospace, nuclear, and mechanical engineering. In this study, the authors focus on calculating the second-moment statistics (Item 1) and PDF (Item 2) of $y(t;\mathbf{X})$ for both simple and complex dynamical systems.

For dynamics of continuous media with domain $\mathcal{D} \subset \mathbb{R}^d$, $d = 1,2,3$, a more general version of Eq. (1), representing space–time SDEs as governing equations, should be considered. In such cases, the time-dependent UQ problem further generalizes to solving

$$\begin{aligned} \mathcal{A}\left[\mathbf{y}(\mathbf{u},t;\mathbf{X})\right] &= g(\mathbf{u},t;\mathbf{X}),\ \mathbf{u}\in\mathcal{D}\subset\mathbb{R}^d,\ t\in[0,T]\subseteq\mathbb{R}_0^+,\\ &\quad \mathbf{y}\in L^2(\Omega,\mathcal{F},P),\\ \mathcal{B}\left[\mathbf{y}(\mathbf{u},t;\mathbf{X})\right] &= 0,\\ \mathcal{C}\left[\mathbf{y}(\mathbf{u},0;\mathbf{X})\right] &= q(\mathbf{X}), \end{aligned} \tag{2}$$

where the excitation $g(\mathbf{u},t;\mathbf{X})$ and dynamic response $\mathbf{y}(\mathbf{u},t;\mathbf{X})$ also depends on a spatial coordinate $\mathbf{u}\in\mathcal{D}\subset\mathbb{R}^d$ and $\mathcal{B}$ is an appropriate boundary condition operator. Here, the domain $\mathcal{D}$ must be discretized spatially using the finite-element or other numerical methods. Domain discretizations requiring thousands or millions of degrees of freedom are not uncommon. Therefore, UQ for space–time-dependent complex problems is a vastly expensive initiative.

In this paper, the proposed PDD-NARX approximation is described in the context of solving a general time-dependent UQ problem represented by Eq. (1). The solution of Eq. (2) is similar and will be dealt with in the Application section. The exposition involves (1) a stochastic adaptation of NARX to accurately capture the underlying dynamical system behavior; (2) a PDD approximation of random coefficients generated by NARX; and (3) a new integration between NARX and PDD, establishing the PDD-NARX approximation.

3. Stochastic NARX

Consider a general system identification problem aimed at building a mathematical model to describe approximately the output response $y(t;\mathbf{X})$ of a time-dependent or dynamic system subject to the input excitation $g(t;\mathbf{X})$. Using the observed or calculated data of the input and output signals, such approximation allows one to determine the output function $y(t;\mathbf{X})$ without directly solving Eq. (1) at a time t of interest.

3.1. NARX approximation

Given a time interval $[0,T]$, $T\in[0,\infty)$, and a chosen integer $J\in\mathbb{N}$, let

$$0 = t_0 < t_1 < \cdots < t_J = T < \infty,\ t_j\in[0,T],\ j = 0,1,\dots,J,$$

be $(J+1)$ discrete time instants with the constant time step $\Delta t = t_j - t_{j-1}, j = 1,\dots,J$. The uniform spacing of discrete times is merely for simplicity, as variable time steps can be handled rather easily. At these discrete times, the input excitations, if they exist, are

$$g(t_0;\mathbf{X}), g(t_1;\mathbf{X}), \dots, g(t_J;\mathbf{X})$$

and the output responses are

$$y(t_0;\mathbf{X}), y(t_1;\mathbf{X}), \dots, y(t_J;\mathbf{X}),$$

where the latter are either measured or calculated, for instance, by solving Eq. (1). According to NARX [16,18], the dynamic response $y(t_j;\mathbf{X})$ at a current time t_j is approximated by

$$\begin{aligned} \tilde{y}(t_j;\mathbf{X}) = F\big(&g(t_j;\mathbf{X}), g(t_j-\Delta t;\mathbf{X}), \dots, g(t_j - n_g\Delta t;\mathbf{X}),\\ &y(t_j-\Delta t;\mathbf{X}), \dots, y(t_j - n_y\Delta t;\mathbf{X})\big), \end{aligned} \tag{3}$$

which depends on the excitation $g(t_j;\mathbf{X})$ at the current time t_j and pairs of lagged excitations and system responses from the past determined by the respective maximum numbers $n_g\in\mathbb{N}$ and $n_y\in\mathbb{N}$ of time lags and the NARX model function F to be ascertained.[3] Denote by

$$\begin{aligned} \mathbf{z}(t_j;\mathbf{X}) := \big\{&g(t_j;\mathbf{X}), g(t_j-\Delta t;\mathbf{X}), \dots, g(t_j - n_g\Delta t;\mathbf{X}),\\ &y(t_j-\Delta t;\mathbf{X}), \dots, y(t_j - n_y\Delta t;\mathbf{X})\big\}^{\mathsf{T}} \end{aligned} \tag{4}$$

an M-dimensional (say) vector of input–output pairs consisting of such system excitations and responses. If there are no external excitations, then $\mathbf{z}(t_j;\mathbf{X})$ comprises only response states included in Eq. (3). Then the NARX approximation in Eq. (3) can be succinctly written as

$$\tilde{y}(t_j;\mathbf{X}) = F\left(\mathbf{z}(t_j;\mathbf{X})\right). \tag{5}$$

It is obvious that the approximation quality of $\tilde{y}(t_j;\mathbf{X})$ depends on how the model function $F(\mathbf{z}(t_j;\mathbf{X}))$ is determined. In addition, the underlying form of $F(\mathbf{z}(t_j;\mathbf{X}))$ must be suitably nonlinear to capture the actual nonlinearity of a dynamical system.

According to Eq. (3) or Eq. (4), the NARX approximation is grounded on a finite memory model, well-recognized by the system identification community, when analyzing dynamical system responses in practical applications [16]. As a result, the NARX approximation sidesteps the need for expensive calculation of $y(t_j;\mathbf{X})$ from Eq. (1) directly, but it still captures the dynamical system behavior by following the principle of causality; that is, the current state of the system $y(t_j;\mathbf{X})$ is influenced by its previous states

$$y(t_j-\Delta t;\mathbf{X}), \dots, y(t_j - n_y\Delta t;\mathbf{X})$$

and external excitations

$$g(t_j;\mathbf{X}), g(t_j-\Delta t;\mathbf{X}), \dots, g(t_j - n_g\Delta t;\mathbf{X})$$

at current and previous states, if they exist. As will be shown later, only a smaller subset of dynamic time histories is needed to calibrate the NARX approximation. Depending on how fast the cause-consequence effects decay as time evolves, a small or large value of M will be required. If M is small, then Eq. (3) or Eq. (5) is effective. However, if M is large, then there will be too many basis functions involved, although not all basis functions are important or needed. These issues are discussed in the following subsection.

[3] Strictly speaking, Eq. (3) is valid when $t_j > n_g\Delta t$ and/or $t_j > n_y\Delta t$. Otherwise, appropriate modifications are required to avoid negative time instants.

3.2. Construction of NARX model function

An effective construction of the NARX model function $F(\mathbf{z}(t_j;\mathbf{X}))$ relies on how it is expanded with respect to its argument $\mathbf{z}(t_j;\mathbf{X})$. Denote by $z_i(t_j;\mathbf{X})$ the ith component of $\mathbf{z}(t_j;\mathbf{X})$. There are M such components, depending on the chosen numbers of time lags n_g and n_y. For instance, when $n_g = n_y = 4$, then, according to Eq. (4), $M = 9$. Here, two types of expansion are described as follows.

3.2.1. Full tensor-product expansion

For each component variable $z_i(t_j;\mathbf{X})$, $i = 1,\dots,M$, and $m' \in \mathbb{N}$, let

$$\{\phi_{i,0}(z_i(t_j;\mathbf{X})), \phi_{i,1}(z_i(t_j;\mathbf{X})), \dots, \phi_{i,m'}(z_k(t_j;\mathbf{X}))\}, \phi_{i,0}(z_i(t_j;\mathbf{X})) = 1,$$

be a set of $(m'+1)$ univariate basis functions. Here, $\phi_{i,j_i}(z_i(t_j;\mathbf{X}))$ is referred to as the j_ith-order univariate basis function. More specifically, the authors propose to use an m'th-order monomial basis vector

$$\{1, z_i(t_j;\mathbf{X}), z_i^2(t_j;\mathbf{X}) \dots, z_i^{m'}(t_j;\mathbf{X})\}^\intercal,\ i = 1,\dots,M,\ m' \in \mathbb{N},$$

with respect to $z_i(t_j;\mathbf{X})$. For instance, if a second-order ($m' = 2$) monomial basis vector is chosen, then there are three basis functions as $m'+1 = 3$. These basis functions are random because $F(\mathbf{z}(t_j;\mathbf{X}))$ is random.

Define an M-dimensional multi-index $\mathbf{j} := (j_1,\dots,j_M) \in \mathbb{N}_0^M$, representing the monomial degrees or orders of basis functions in all M components of $\mathbf{z}(t_j;\mathbf{X})$.[4] Each element j_i, $i = 1,\dots,M$, of the multi-index runs from *zero* to m', the largest degree or order retained in the monomial basis vector. Then, there exists $(m'+1)^M$ multivariate basis functions

$$\boldsymbol{\Phi}_{\mathbf{j}}(\mathbf{z}(t_j;\mathbf{X})) = \prod_{i=1}^{M} \phi_{i,j_i}(z_i(t_j;\mathbf{X})), \tag{6}$$

obtained using an M-dimensional or full tensor product of univariate basis functions. Therefore, the model function $F(\mathbf{z}(t_j;\mathbf{X}))$ can be expanded with respect to such a multivariate basis, resulting in the approximation

$$\tilde{y}(t_j;\mathbf{X}) \simeq \sum_{\substack{\mathbf{j}\in\mathbb{N}_0^M \\ \max_{i=1,\dots,M} j_i \le m'}} R_{\mathbf{j}}(\mathbf{X})\boldsymbol{\Phi}_{\mathbf{j}}(\mathbf{z}(t_j;\mathbf{X})), \tag{7}$$

where

$$R_{\mathbf{j}}(\mathbf{X}),\ \{\mathbf{j}\in\mathbb{N}_0^M\ :\ \max_{i=1,\dots,M} j_i \le m'\},$$

are the corresponding expansion coefficients.

While the construction of multivariate expansion using full tensor product is straightforward, it is not effective when M and/or m' is large. For example, when $M = 9$ and $m' = 2$, there are $(2+1)^9 = 19{,}683$ basis functions already, rendering the resulting NARX approximation computationally prohibitive. More importantly, many of these basis functions are likely unimportant in practical applications and can be safely eliminated without sacrificing accuracy in the NARX approximation.

3.2.2. Dimension-wise tensor-product expansion

For $M \in \mathbb{N}$, let $\{1,\dots,M\}$ be an index set, so that $u \subseteq \{1,\dots,M\}$ is a subset, including the emptyset $\emptyset$, with cardinality $0 \le |u| \le M$. For a non-empty subset $\emptyset \ne u = \{i_1,\dots,i_{|u|}\} \subseteq \{1,\dots,M\}$, denote by

$$\mathbf{z}_u(t_j;\mathbf{X}) = \left\{ z_{i_1}(t_j;\mathbf{X}), \dots, z_{i_{|u|}}(t_j;\mathbf{X}) \right\}^\intercal$$

a $|u|$-dimensional subvector of $\mathbf{z}(t_j;\mathbf{X})$. Then there exists a finite, hierarchical, convergent expansion of

$$F(\mathbf{z}(t_j;\mathbf{X})) = F_\emptyset(\mathbf{X}) + \sum_{\emptyset\ne u\subseteq\{1,\dots,M\}} F_u(\mathbf{z}_u(t_j;\mathbf{X})), \tag{8}$$

known as a general dimensional decomposition of a multivariate function [19–21]. Here, $F_\emptyset(\mathbf{X})$ is a constant, while $F_u(\mathbf{z}_u(t_j;\mathbf{X}))$ is a $|u|$-variate component function describing $|u|$-variate interaction of $\mathbf{z}_u(t_j;\mathbf{X})$ on F. For example, when $u = \{i\}$, $F_{\{i\}}(z_i(t_j;\mathbf{X}))$ is a univariate component function representing individual contribution to $F(\mathbf{z}(t_j;\mathbf{X}))$ by the variable $z_i(t_j;\mathbf{X})$ acting alone. When $u = \{i_1,i_2\}$, $F_{\{i_1,i_2\}}(z_{i_1}(t_j;\mathbf{X}), z_{i_2}(t_j;\mathbf{X}))$ is a bivariate component function representing the interactive effect on $F(\mathbf{z}(t_j;\mathbf{X}))$ by two variables $z_{i_1}(t_j;\mathbf{X})$ and $z_{i_2}(t_j;\mathbf{X})$, and so on. This decomposition is useful when the higher-variate interactive effects become weaker or vanish when $|u| \to M$, as expected in practical applications.

Given an integer $1 \le S' \le M$, an S'-variate approximation, say, $\tilde{F}_{S'}(\mathbf{z}(t_j;\mathbf{X}))$ of $F(\mathbf{z}(t_j;\mathbf{X}))$, is obtained by truncating the right-hand side of Eq. (8), yielding

$$\tilde{F}_{S'}(\mathbf{z}(t_j;\mathbf{X})) = F_\emptyset(\mathbf{X}) + \sum_{\substack{\emptyset\ne u\subseteq\{1,\dots,M\} \\ 1\le|u|\le S'}} F_u(\mathbf{z}_u(t_j;\mathbf{X})). \tag{9}$$

The approximation is coined "S'-variate", as it retains interactive effects on $F(\mathbf{z}(t_j;\mathbf{X}))$ by at most S' variables. In most applications, a univariate ($S' = 1$) or bivariate ($S' = 2$) truncations suffices for such an approximation.

For $\emptyset \ne u \subseteq \{1,\dots,M\}$, let $\mathbf{j}_u := (j_{i_1},\dots,j_{i_{|u|}}) \in \mathbb{N}^{|u|}$ be a $|u|$-dimensional multi-index with degree $\mathbf{j}_u := j_{i_1} + \cdots + j_{i_{|u|}}$, where $j_{i_k} \in \mathbb{N}$, $k = 1,\dots,|u|$, represents the kth element of $\mathbf{j}_u$.[5] Denote by

$$\boldsymbol{\Phi}_{u,\mathbf{j}_u}(\mathbf{z}_u(t_j;\mathbf{X})) = \prod_{k=1}^{|u|} \phi_{i_k,j_{i_k}}(z_{i_k}(t_j;\mathbf{X})) \tag{10}$$

a $|u|$-variate basis function, obtained using a $|u|$-dimensional tensor product of univariate basis functions. Associated with the total-degree index set

$$\left\{ \mathbf{j}_u \in \mathbb{N}^{|u|} \ :\ |\mathbf{j}_u| = \sum_{k=1}^{|u|} j_{i_k} \le m' \right\},$$

there are

$$L'_{S',m'} := 1 + \sum_{s=1}^{S'} \binom{M}{s}\binom{m'}{s} \tag{11}$$

number of such basis functions. Therefore, all $|u|$-variate component functions of $\tilde{F}_{S'}(\mathbf{z}(t_j;\mathbf{X}))$ can be expanded dimension-wise with respect to such a basis, resulting in an S'-variate, m'th-order dimensional decomposition

$$\tilde{y}_{S',m'}(t_j;\mathbf{X}) = F_\emptyset(\mathbf{X}) + \sum_{\substack{\emptyset\ne u\subseteq\{1,\dots,M\} \\ 1\le|u|\le S'}} \sum_{\substack{\mathbf{j}_u\in\mathbb{N}^{|u|} \\ |u|\le|\mathbf{j}_u|\le m'}} R_{u,\mathbf{j}_u}(\mathbf{X})\boldsymbol{\Phi}_{u,\mathbf{j}_u}(\mathbf{z}_u(t_j;\mathbf{X})), \tag{12}$$

of $\tilde{y}(t_j;\mathbf{X})$, where $R_{u,\mathbf{j}_u}(\mathbf{X}) \in \mathbb{R}$, $\emptyset \ne u \subseteq \{1,\dots,M\}$, $\mathbf{j}_u \in \mathbb{N}_0^{|u|}$, are the corresponding expansion coefficients. The number of coefficients, including $F_\emptyset(\mathbf{X})$, is the same as the number of basis functions defined in Eq. (11).

For two special cases of univariate ($S' = 1$) and bivariate ($S' = 2$) approximations, the respective decompositions are

$$\tilde{y}_{1,m'}(t_j;\mathbf{X}) = F_\emptyset(\mathbf{X}) + \sum_{i=1}^{M}\sum_{j_i=1}^{m'} R_{\{i\},j_i}(\mathbf{X})\phi_{i,j_i}(z_i(t_j;\mathbf{X})) \tag{13}$$

and

$$\begin{aligned}\tilde{y}_{2,m'}(t_j;\mathbf{X}) \quad = \quad & F_\emptyset(\mathbf{X}) + \sum_{i=1}^{M}\sum_{j_i=1}^{m'} R_{\{i\},j_i}(\mathbf{X})\phi_{i,j_i}(z_i(t_j;\mathbf{X})) + \\ & \sum_{i_1=1}^{M-1}\sum_{i_2=i_1+1}^{M}\sum_{\substack{j_{i_1},j_{i_2}=1 \\ 2\le j_{i_1}+j_{i_2}\le m'}}^{m'} R_{\{i_1,i_2\},(j_{i_1},j_{i_2})}(\mathbf{X}) \times \\ & \phi_{i_1,j_{i_1}}(z_{i_1}(t_j;\mathbf{X}))\phi_{i_2,j_{i_2}}(z_{i_2}(t_j;\mathbf{X})),\end{aligned} \tag{14}$$

[4] In this paper, the terms degree and order are used interchangeably.

[5] The same symbol $|\cdot|$ is used for denoting both the cardinality of a set and the degree of a multi-index in this paper.

involving

$$L'_{1,m'} = 1 + Mm'$$

and

$$L'_{2,m'} = 1 + Mm' + \frac{M(M-1)}{2}\frac{m'(m'-1)}{2}$$

basis functions or expansion coefficients.

According to Eq. (12), the dimensional decomposition $\tilde{y}_{S',m'}(t_j;\mathbf{X})$ has the potential to markedly reduce the number of basis functions. For example, when $M = 9$, $m' = 2$, and $S' = 1$ or $S' = 2$, there are now $L'_{1,2} = 19$ or $L'_{2,2} = 55$ basis functions, which are substantially lower than 19,683 calculated from the full tensor-product expansion. Therefore, the dimension-wise tensor-product expansion renders the resulting NARX approximations computationally feasible, provided that the degree of interaction S' and order of basis functions m' are judiciously selected.

Note that the NARX approximation in Eq. (12) is stochastic and distinguished from the classical NARX approximation due to the fact that the model coefficients $F_{\emptyset}(\mathbf{X})$ and $R_{u,\mathbf{j}_u}(\mathbf{X})$, instead of being deterministic constants, are now functions of random parameters $\mathbf{X}$. As described in a following section, the stochastic NARX proposed facilitates propagation of input uncertainties using any preferred method of UQ analysis.

3.2.3. Reduction of no. of NARX basis functions

While a dimension-wise construction of NARX model function produces a huge decrease in the number of basis functions already, a further reduction is possible if the coefficients corresponding to some of the basis functions are negligibly small. However, as the NARX expansion coefficients $R_{u,\mathbf{j}_u}(\mathbf{X})$ are functions of input random variables, the magnitude of smallness must be determined in a statistical sense. A four-step algorithm is proposed for basis reduction, as follows.

1. Given the known probability distribution of $\mathbf{X}$, generate $\{\mathbf{x}^{(l)}\}_{l=1,\dots,L'}$, a set of associated samples of input random variables of size $L' \in \mathbb{N}$.
2. For each input sample $\mathbf{x}^{(l)}$, conduct an appropriate regression analysis by fitting an S'-variate, m'th-order approximation $\tilde{y}_{S',m'}(t_j;\mathbf{x}^{(l)})$ to the original function $y(t_j;\mathbf{x}^{(l)})$, thereby obtaining the corresponding sample of NARX expansion coefficients $R_{u,\mathbf{j}_u}(\mathbf{x}^{(l)})$. More specific details of such regression analysis will be provided in a forthcoming section.
3. Determine the importance of the NARX basis function $\Phi_{u,\mathbf{j}_u}(\mathbf{z}_u(t_j;\mathbf{X}))$ by estimating the mean of the NARX coefficient $R_{u,\mathbf{j}_u}(\mathbf{X})$, referred to as the importance factor, from

$$\bar{\alpha}_{u,\mathbf{j}_u} := \frac{1}{L'}\sum_{l=1}^{L'} \frac{R^2_{u,\mathbf{j}_u}(\mathbf{x}^{(l)})}{\sum_{\substack{\emptyset\neq u\subseteq\{1,\dots,M\}\\ 1\le|u|\le S'}}\ \sum_{\substack{\mathbf{j}_u\in\mathbb{N}^{|u|}\\ |u|\le|\mathbf{j}_u|\le m'}} R^2_{u,\mathbf{j}_u}(\mathbf{x}^{(l)})}. \tag{15}$$

   According to Eq. (15), the lower the value of $\bar{\alpha}_{u,\mathbf{j}_u}$, the less important the corresponding basis function $\Phi_{u,\mathbf{j}_u}(\mathbf{z}_u(t_j;\mathbf{X}))$.
4. Define a threshold parameter $0 \le \alpha_0 \le 1$ for grading the values of $\bar{\alpha}_{u,\mathbf{j}_u}$ from (15). Thereby, remove all basis functions when their importance factors are less than the threshold, that is, from the condition: $\bar{\alpha}_{u,\mathbf{j}_u} \le \alpha_0$.

Fig. 1 shows the computational flow of the four-step algorithm. Compared with past works where the basis functions are chosen ad-hoc or intuitively [18], the proposed algorithm illustrates how the dimensional decomposition in tandem with the importance factor can be exploited for a more systematic way of constructing the NARX model function $F(\mathbf{z}(t_j;\mathbf{X}))$.

It is important to recognize that the magnitude of reduction in the number of NARX basis functions from the proposed algorithm depends on the values of S', m', and α_0 chosen by a user. Furthermore, the reduction also depends on the behavior of original NARX model function $F(\mathbf{z}(t_j;\mathbf{X}))$. Nonetheless, in practice, a huge reduction is possible, to be demonstrated in the Examples and Application sections.

3.3. Estimation of NARX coefficients

As alluded to earlier, the NARX coefficients are random. Therefore, a UQ method is needed for their statistical characterization. Here, the coefficients are determined in terms of their samples using standard least-square (SLS) regression. Such sample values are required for basis reduction, as explained in Section 3.2. In addition, these sample values will also be needed when PDD is introduced for UQ analysis in Section 4.

When applying SLS or other regression methods, expressing the NARX approximation in terms of a single index is beneficial. In this case, arrange the elements of the sets of NARX basis and coefficients by

$$\{\phi_1(\mathbf{z}(t_j;\mathbf{x}^{(l)})),\dots,\phi_{L'_{S',m'}}(\mathbf{z}(t_j;\mathbf{x}^{(l)}))\} \text{ and } \{R_1(\mathbf{x}^{(l)}),\dots,R_{L'_{S',m'}}(\mathbf{x}^{(l)})\},$$

respectively, where $L'_{S',m'}$ is the total number of basis functions determined from the dimensional decomposition parameters S' and m' of the NARX model function and $\mathbf{x}^{(l)}$ is an lth sample, also known as realization or experiment, of $\mathbf{X}$, generated from the known probability distribution of random input. Here, $L'_{S',m'}$ may represent either an unreduced number of basis functions from a dimensional decomposition or a reduced number of such basis functions via removal of unimportant basis functions from the proposed four-step algorithm. The subsequent regression analysis is the same. However, in the Example and Application sections, $L'_{S',m'}$ will represent the final, reduced number of basis functions to demonstrate the effectiveness of the algorithm.

Given an $L'_{S',m'}$ number of basis functions, the NARX approximation can also be expressed by

$$\tilde{y}_{S',m'}(t_j;\mathbf{X}) = \sum_{i=1}^{L'_{S',m'}} R_i(\mathbf{X})\Phi_i(\mathbf{z}(t_j;\mathbf{X})). \tag{16}$$

Denote by $y(t_j;\mathbf{x}^{(l)})$, $\mathbf{z}(t_j;\mathbf{x}^{(l)})$, and $\tilde{y}(t_j;\mathbf{x}^{(l)})$ the lth samples of $y(t_j;\mathbf{X})$, $\mathbf{z}(t_j;\mathbf{X})$, and $\tilde{y}(t_j;\mathbf{X})$, respectively. Then, employing SLS regression, the coefficients of the NARX approximation for this particular sample are obtained by minimizing the sum of squared errors,

$$\begin{aligned} e_{\text{NARX}} &:= \sum_{j=0}^{J}\left[y(t_j;\mathbf{x}^{(l)}) - \tilde{y}_{S',m'}(t_j;\mathbf{x}^{(l)})\right]^2 \\ &= \sum_{j=0}^{J}\left[y(t_j;\mathbf{x}^{(l)}) - \sum_{i=1}^{L'_{S',m'}} R_i(\mathbf{X})\Phi_i(\mathbf{z}(t_j;\mathbf{x}^{(l)}))\right]^2, \end{aligned} \tag{17}$$

committed by NARX at all $(J+1)$ time instants t_j, $j = 0,\dots,J$. The minimization leads to a sample of approximate NARX coefficients

$$\tilde{\mathbf{R}}(\mathbf{x}^{(l)}) := \left\{\tilde{R}_1(\mathbf{x}^{(l)}),\dots,\tilde{R}_{L'_{S',m'}}(\mathbf{x}^{(l)})\right\}^{\intercal} = (\mathbf{A}_l^{\intercal}\mathbf{A}_l)^{-1}\mathbf{A}_l^{\intercal}\mathbf{b}_l, \tag{18}$$

where

$$\mathbf{A}_l := \begin{bmatrix} \phi_1(\mathbf{z}(t_0;\mathbf{x}^{(l)})) & \cdots & \phi_{L'_{S',m'}}(\mathbf{z}(t_0;\mathbf{x}^{(l)})) \\ \vdots & \ddots & \vdots \\ \phi_1(\mathbf{z}(t_J;\mathbf{x}^{(l)})) & \cdots & \phi_{L'_{S',m'}}(\mathbf{z}(t_J;\mathbf{x}^{(l)})) \end{bmatrix} \tag{19}$$

and

$$\mathbf{b}_l := \{y(t_0;\mathbf{x}^{(l)}),\dots,y(t_J;\mathbf{x}^{(l)})\}^{\intercal} \tag{20}$$

are a $(J+1)\times L'_{S',m'}$ matrix comprising values of NARX basis functions at discrete time instants and an $(J+1)$-dimensional column vector containing values of output response function at time instants, respectively. In Eq. (18), $\mathbf{A}_l^{\intercal}\mathbf{A}_l$ is an $L'_{S',m'}\times L'_{S',m'}$ matrix, often referred to as the information or data matrix.

The estimated NARX coefficients $\tilde{\mathbf{R}}(\mathbf{x}^{(l)})$ obtained from Eq. (18) should improve if the time step Δt decreases. Moreover, when $S' \to M$ and $m' \to \infty$, the NARX approximation $\tilde{y}_{S',m'}(t_j;\mathbf{x}^{(l)})$ should approach the exact function $y(t_j;\mathbf{x}^{(l)})$ in the mean-square sense.

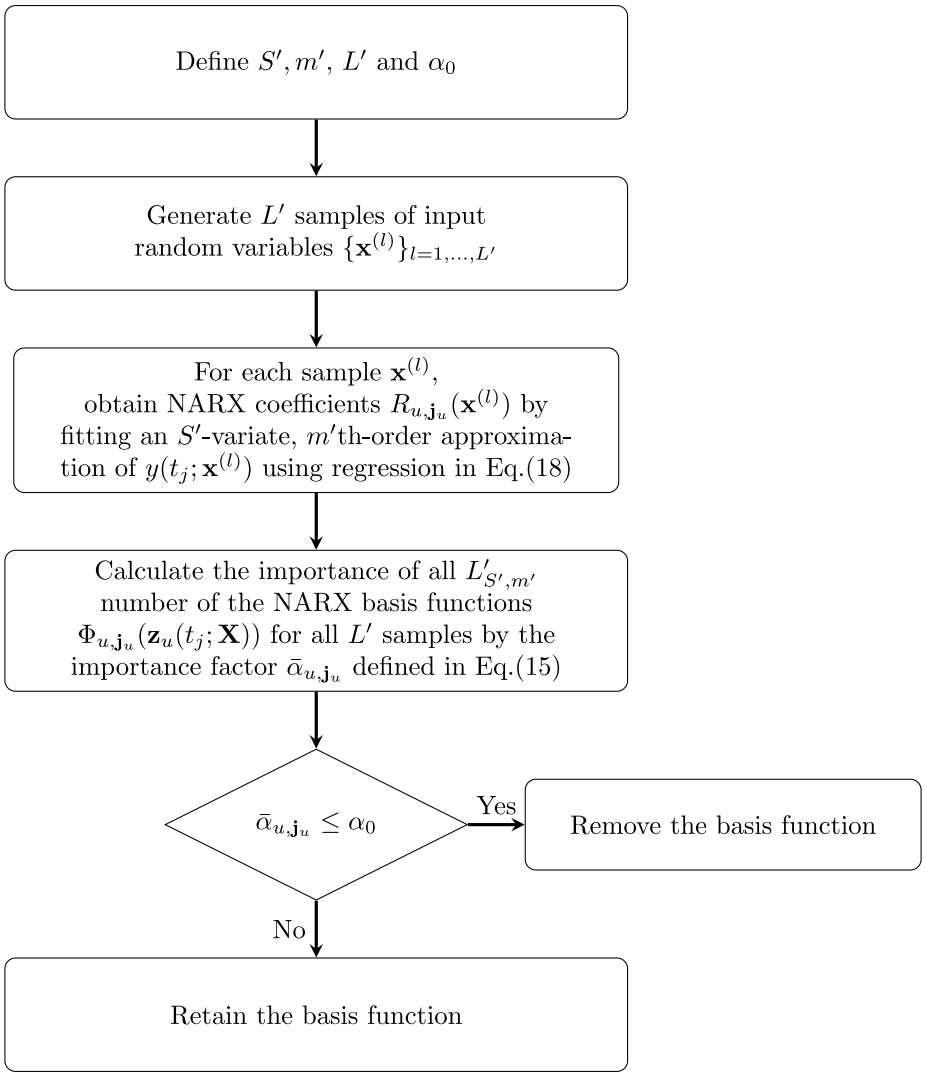

Fig. 1. A four-step algorithm for reducing the number of NARX basis functions.

4. PDD

Given an input random vector $\mathbf{X} := \{X_1, \dots, X_N\}^T : (\Omega, \mathcal{F}) \to (\mathbb{A}^N, \mathcal{B}^N)$ with known PDF $f_{\mathbf{X}}(\mathbf{x})$, let the NARX coefficients $R_i(\mathbf{X}) := R_i(X_1, \dots, X_N)$, $i = 1, \dots, L_{\text{NARX}}$ – a real-valued, measurable transformation on $(\Omega, \mathcal{F})$ – describe a stochastic response function of interest. It is common to assume that the function $R_i(\mathbf{X})$ belongs to a reasonably large function class, such as the Hilbert space

$$L^2(\Omega, \mathcal{F}, \mathbb{P}) := \left\{ R_i : \Omega \to \mathbb{A} : \int_\Omega \left| R_i(\mathbf{X}(\omega)) \right|^2 d\mathbb{P}(\omega) < \infty \right\}, \tag{21}$$

with respect to the probability measure $f_{\mathbf{X}}(\mathbf{x})d\mathbf{x}$. A principal objective of UQ analysis is to effectively estimate the relevant probabilistic characteristics of $R_i(\mathbf{X}) \in L^2(\Omega, \mathcal{F}, \mathbb{P})$. In this work, the authors advocate PDD for such UQ analysis, described as follows.

4.1. ANOVA dimensional decomposition

Following similar considerations in Section 3.2.2, denote by u a subset of the index set $\{1, \dots, N\}$ with the complementary set $-u := \{1, \dots, N\} \backslash u$ and cardinality $0 \le |u| \le N$. For $\emptyset \ne u \subseteq \{1, \dots, N\}$, let $\mathbf{X}_u = \{X_{i_1}, \dots, X_{i_{|u|}}\}^\intercal$, $1 \le i_1 < \cdots < i_{|u|} \le N$, be a subvector of $\mathbf{X}$ with $\mathbf{X}_{-u} := \mathbf{X}_{\{1,\dots,N\}\backslash u}$ defining its complementary subvector. Then, for a given $\emptyset \ne u \subseteq \{1, \dots, N\}$, the marginal density function of $\mathbf{X}_u$, defined on $\mathbb{A}^{|u|} := \times_{k=1}^{|u|}(a_{i_k}, b_{i_k})$, is

$$f_{\mathbf{X}_u}(\mathbf{x}_u) := \int_{\mathbb{A}^{-u}} f_{\mathbf{X}}(\mathbf{x}) d\mathbf{x}_{-u} = \prod_{k=1}^{|u|} f_{X_{i_k}}(x_{i_k}), \tag{22}$$

where the second equality forms due to statistical independence of the input random variables as per Assumption 1. Hence, it can be shown that, for any function $R_i(\mathbf{X}) \in L^2(\Omega, \mathcal{F}, \mathbb{P})$, there exists a unique, finite, hierarchical expansion [19–22]

$$R_i(\mathbf{X}) = R_{i,\emptyset} + \sum_{\emptyset \ne u \subseteq \{1,\dots,N\}} R_{i,u}(\mathbf{X}_u), \tag{23a}$$

$$R_{i,\emptyset} := \int_{\mathbb{A}^N} R_i(\mathbf{x}) f_{\mathbf{X}}(\mathbf{x}) d\mathbf{x}, \tag{23b}$$

$$R_{i,u}(\mathbf{X}_u) := \int_{\mathbb{A}^{-u}} R_i(\mathbf{X}_u, \mathbf{x}_{-u}) f_{\mathbf{X}_{-u}}(\mathbf{x}_{-u}) d\mathbf{x}_{-u} - \sum_{v \subset u} R_{i,v}(\mathbf{X}_v), \tag{23c}$$

referred to as the ANOVA dimensional decomposition (ADD), where $R_{i,u}$ is a $|u|$-variate component function describing a constant or an $|u|$-variate interaction of $\mathbf{X}_u = (X_{i_1}, \dots, X_{i_{|u|}})$ on R_i when $|u| = 0$ or $|u| > 0$. Here, $(\mathbf{X}_u, \mathbf{x}_{-u})$ denotes an N-dimensional vector whose kth component is X_{i_k} if $i_k \in u$ and x_{i_k} if $i_k \notin u$. The summation in Eq. (23a) comprises $2^N - 1$ terms with each term depending on a group of variables indexed by a particular subset of $\{1, \dots, N\}$.

The ADD described by Eqs. (23a)–(23c) is a special type of dimensional decomposition presented earlier. Such ADD has two notable properties [20]:

1. Any non-constant component function $R_{i,u}(\mathbf{X}_u)$ has a *zero* mean, that is,
$$\mathbb{E}[R_{i,u}(\mathbf{X}_u)] = 0,\ \emptyset \neq u \in \{1,\dots,N\}. \tag{24}$$
2. Any two distinct component functions $R_{i,u}(\mathbf{X}_u)$ and $R_v(\mathbf{X}_{i,v})$ are mutually orthogonal, that is,
$$\mathbb{E}[R_{i,u}(\mathbf{X}_u)R_{i,v}(\mathbf{X}_v)] = 0,\ u,v \in \{1,\dots,N\},\ u \neq v. \tag{25}$$

Readers interested in further details of ADD are directed to the authors' prior work [20].

It is elementary to show that all ADD component functions of $R_i(\mathbf{X})$ are members of respective subspaces of $L^2(\Omega,\mathcal{F},\mathbb{P})$. Unfortunately, the subspaces are infinite-dimensional. Therefore, a further discretization or refinement is necessary. In this work, the authors propose to employ polynomial refinements, leading to PDD approximation of $R_i(\mathbf{X})$.

4.2. Measure-consistent orthonormal polynomials

Let $\{\psi_{ij}(X_i) : j = 0,1,\dots\}$ be a set of univariate, orthonormal polynomial basis functions in the Hilbert space $L^2(\Omega_i,\mathcal{F}_i,P_i)$ that is consistent with the probability measure P_i or $f_{X_i}(x_i)dx_i$ of X_i. For $\emptyset \neq u = \{i_1,\dots,i_{|u|}\} \subseteq \{1,\dots,N\}$, where $1 \leq |u| \leq N$ and $1 \leq i_1 < \cdots < i_{|u|} \leq N$, let

$$\left(\times_{k=1}^{k=|u|}\Omega_{i_k}, \times_{k=1}^{k=|u|}\mathcal{F}_{i_k}, \times_{k=1}^{k=|u|}P_{i_k}\right)$$

be the product probability triple of $\mathbf{X}_u = \{X_{i_1},\dots,X_{i_{|u|}}\}^\intercal$. Denote the associated space of the $|u|$-variate component functions of R_i by

$$L^2\left(\times_{k=1}^{k=|u|}\Omega_{i_k}, \times_{k=1}^{k=|u|}\mathcal{F}_{i_k}, \times_{k=1}^{k=|u|}P_{i_k}\right) := \left\{R_{i,u} : \int_{\mathbb{A}^{|u|}} R_{i,u}^2(\mathbf{x}_u) f_{\mathbf{X}_u}(\mathbf{x}_u)d\mathbf{x}_u < \infty\right\},$$

which is also a Hilbert space. Since the input random variables are statistically independent (Assumption 1), the joint density of $\mathbf{X}_u$ is separable, that is,

$$f_{\mathbf{X}_u}(\mathbf{x}_u) = \prod_{k=1}^{|u|} f_{X_{i_k}}(x_{i_k}),$$

the product

$$\psi_{u,\mathbf{j}_u}(\mathbf{X}_u) := \prod_{k=1}^{|u|} \psi_{i_k j_k}(X_{i_k}),$$

where $\mathbf{j}_u = (j_1,\dots,j_{|u|}) \in \mathbb{N}_0^{|u|}$, a $|u|$-dimensional multi-index, constitutes a measure-consistent multivariate orthonormal polynomial basis of

$$L^2\left(\times_{k=1}^{k=|u|}\Omega_{i_k}, \times_{k=1}^{k=|u|}\mathcal{F}_{i_k}, \times_{k=1}^{k=|u|}P_{i_k}\right).$$

Two important properties of these multivariate orthonormal polynomials are as follows [7,8]:

1. The polynomials $\psi_{u,\mathbf{j}_u}(\mathbf{X}_u)$, $\emptyset \neq u \subseteq \{1,\dots,N\}$, $j_1,\dots,j_{|u|} \neq 0$, have zero means, i.e.,
$$\mathbb{E}\left[\psi_{u,\mathbf{j}_u}(\mathbf{X}_u)\right] = 0. \tag{26}$$
2. Any two distinct polynomials $\psi_{u,\mathbf{j}_u}(\mathbf{X}_u)$ and $\psi_{v,\mathbf{k}_v}(\mathbf{X}_v)$, where $\emptyset \neq u \subseteq \{1,\dots,N\}$, $\emptyset \neq v \subseteq \{1,\dots,N\}$, $\mathbf{j}_u = (j_1,\dots,j_{|u|}) \neq 0$, $\mathbf{k}_v = (k_1,\dots,k_{|v|}) \neq 0$, are uncorrelated and each has unit variance, i.e.,
$$\mathbb{E}\left[\psi_{u,\mathbf{j}_u}(\mathbf{X}_u)\psi_{v,\mathbf{k}_v}(\mathbf{X}_v)\right] = \begin{cases} 1 & \text{if } u = v; \mathbf{j}_{|u|} = \mathbf{k}_{|v|}, \\ 0 & \text{otherwise.} \end{cases} \tag{27}$$

Given a probability measure P_{i_k} or $f_{X_{i_k}}(x_{i_k})dx_{i_k}$ of X_{i_k} of a random variable X_{i_k}, the well-known three-term recurrence relation is commonly used to construct the associated orthogonal polynomials [23]. The recursion coefficients lead to general orthogonal polynomials, including classical orthogonal polynomials, such as Hermite, Legendre, and Jacobi polynomials, when X_{i_k} follows the Gaussian, uniform, and Beta probability distributions, respectively. For an arbitrary probability measure, the Stieltjes procedure can be employed to obtain the recursion coefficients and associated orthogonal polynomials approximately [23,24].

4.3. PDD approximation

The PDD of a square-integrable random variable $R_i(\mathbf{X}) \in L^2(\Omega,\mathcal{F},\mathbb{P})$ is simply the expansion of $R_i(\mathbf{X})$ with respect to a complete, hierarchically ordered, orthonormal polynomial basis of $L^2(\Omega,\mathcal{F},\mathbb{P})$. It involves the following two steps: (1) expand the ADD component function

$$R_{i,u}(\mathbf{X}_u) = \sum_{\mathbf{j}_u \in \mathbb{N}^{|u|}} C_{i,u,\mathbf{j}_u}\Psi_{u,\mathbf{j}_u}(\mathbf{X}_u) \tag{28}$$

in terms of the measure-consistent orthonormal basis with $C_{i,u,\mathbf{j}_u}$, $\emptyset \neq u \subseteq \{1,\dots,N\}$, $\mathbf{j}_u \in \mathbb{N}^{|u|}$, representing the associated expansion coefficients; and (2) apply Eq. (28) to Eq. (23a) and exploit orthogonal properties of the basis. The end result is the PDD [7,8] of

$$R_i(\mathbf{X}) = R_{i,\emptyset} + \sum_{\emptyset \neq u \subseteq \{1,\dots,N\}} \sum_{\mathbf{j}_u \in \mathbb{N}^{|u|}} C_{i,u,\mathbf{j}_u}\Psi_{u,\mathbf{j}_u}(\mathbf{X}_u), \tag{29}$$

where, eventually,

$$C_{i,u,\mathbf{j}_u} = \int_{\mathbb{A}^N} R_i(\mathbf{x})\Psi_{u,\mathbf{j}_u}(\mathbf{x}_u) f_{\mathbf{X}}(\mathbf{x})d\mathbf{x}. \tag{30}$$

Comparing Eqs. (29) and (23a), the connection between PDD and ADD is clearly palpable, where the former can be viewed as a polynomial variant of the latter. For instance, $C_{i,u,\mathbf{j}_u}\Psi_{u,\mathbf{j}_u}(\mathbf{X}_u)$ in Eq. (29) represents a $|u|$-variate, $|\mathbf{j}_u|$th-order PDD component function of $R_i(\mathbf{X})$, describing the $|\mathbf{j}_u|$th-order polynomial approximation of $R_{i,u}(\mathbf{X}_u)$. In addition, PDD inherits all desirable properties of ADD [8].

The full PDD contains an infinite number of orthonormal polynomials or coefficients. In practice, the number must be finite, meaning that PDD must be truncated. In a practical setting, the function $R_i(\mathbf{X})$ is likely to have an effective dimension much lower than N, meaning that the right side of Eq. (29) can be effectively truncated by a sum of lower-dimensional component functions of PDD, but still preserve all random variables $\mathbf{X}$ of a high-dimensional UQ problem. A straightforward approach adopted in this work entails (1) keeping all polynomials in at most $0 \leq S \leq N$ variables, thereby retaining the degrees of interaction among input variables less than or equal to S and (2) preserving polynomial expansion orders (total) less than or equal to $S \leq m < \infty$. The result is an S-variate, mth-order PDD approximation

$$\tilde{R}_{i,S,m}(\mathbf{X}) = R_{i,\emptyset} + \sum_{\substack{\emptyset \neq u \subseteq \{1,\dots,N\} \\ 1 \leq |u| \leq S}} \sum_{\substack{\mathbf{j}_u \in \mathbb{N}^{|u|} \\ |u| \leq |\mathbf{j}_u| \leq m}} C_{i,u,\mathbf{j}_u}\Psi_{u,\mathbf{j}_u}(\mathbf{X}_u) \tag{31}$$

of $R_i(\mathbf{X})$, containing

$$L_{S,m} = 1 + \sum_{s=1}^{S} \binom{N}{s}\binom{m}{s} \tag{32}$$

number of expansion coefficients, including $R_{i,\emptyset}$. It is important to clarify a few things about the truncated PDD. First, the right side of Eq. (31) contains sums of at most S-dimensional orthonormal polynomials, representing at most S-variate PDD component functions of R_i. Therefore, the term "S-variate" used for the PDD approximation should be interpreted in the context of including at most S-degree interaction of input variables, even though $\tilde{R}_{i,S,m}$ is strictly an N-variate function. Second, when $S = 0$, $\tilde{R}_{i,0,m} = R_{i,\emptyset}$ for any m as the outer sum of Eq. (31) vanish. Finally, when $S \to N$ and $m \to \infty$, $\tilde{R}_{i,S,m}$ converges to R_i in the mean-square sense, generating a hierarchical and convergent sequence of PDD approximations. Third, if $S \ll N$, as it is anticipated to hold in real-life applications, the number of PDD's basis functions drops

precipitously, ushering in substantial savings of computational effort. Readers interested in an adaptive version of PDD, where the truncation parameters are automatically chosen, are directed to the work of Yadav and Rahman [25], including an application to design optimization [26].

4.4. Estimation of PDD coefficients

The determination of the PDD coefficients $R_{i,\emptyset}$ and $C_{i,u,\mathbf{j}_u}$ involves various N-dimensional integrations. For an arbitrary function $R_i(\mathbf{X})$ and an arbitrary probability distribution of random input $\mathbf{X}$, an exact evaluation of these coefficients from definition alone is impossible. For a high-dimensional problem, say, with N exceeding 10, evaluating the N-dimensional integral numerically is computationally formidable and likely prohibitive. Therefore, a practical alternative to numerical integration, such as regression analysis, is often necessary to estimate these coefficients.

While the compact notations used in Eq. (31) enable a concise description of PDD, a version using a single index notation is better suited for calculating the PDD coefficients as well. Following similar arrangements of NARX basis and coefficients, organize the elements of the sets of PDD basis and coefficients

$$\left\{\Psi_{u,\mathbf{j}_u}(\mathbf{X}_u)\right\}_{1\le|u|\le S,\,|u|\le|\mathbf{j}_u|\le m} \text{ and } \left\{C_{i,u,\mathbf{j}_u}(\mathbf{X}_u)\right\}_{1\le|u|\le S,\,|u|\le|\mathbf{j}_u|\le m}$$

by

$$\{\Psi_1(\mathbf{X}),\dots,\Psi_{L_{S,m}}(\mathbf{X})\} \text{ and } \{C_{i,1},\dots,C_{i,L_{S,m}}\},$$

respectively. As a result, the S-variate, mth order PDD approximation can also be written as

$$\tilde{R}_{i,S,m}(\mathbf{X}) = \sum_{k=1}^{L_{S,m}} C_{i,k}\Psi_k(\mathbf{X}), \tag{33}$$

with the expansion coefficients

$$C_{i,k} = \int_{\mathbb{A}^N} R_{i,S,m}(\mathbf{x})\Psi_k(\mathbf{x})f_{\mathbf{X}}(\mathbf{x})d\mathbf{x},\ \ k=1,\dots,L_{S,m}. \tag{34}$$

The SLS regression is founded on the optimal approximation quality of the PDD approximation. Given the function $R_i(\mathbf{X})$, select a sample size $L\in\mathbb{N}$ and draw input samples $\mathbf{x}^{(l)}$, $l=1,\dots,L$, from the known distribution of random input $\mathbf{X}$. Various sampling methods, namely, standard MCS, quasi MCS, and Latin hypercube sampling, can be used. Corresponding to each input sample, perform full-scale dynamic analysis by solving Eq. (1), thus producing L sets of the dynamic responses. Therefore, L should be as small as possible, enabling such repeated dynamic analyses computationally feasible. From these samples of dynamic responses, often referred to as training data, along with the corresponding samples of excitation time series, generate the data set

$$\left\{\mathbf{x}^{(l)}, R_i(\mathbf{x}^{(l)})\right\}_{l=1}^{L},$$

where $R_i(\mathbf{x}^{(l)})$ is the lth sample of the NARX coefficient $R_i(\mathbf{X})$, the evaluation of which is already described in a previous section. According to SLS, the expansion coefficients of an S-variate, mth-order PDD approximation are estimated by minimizing the empirical analog of the mean-square error

$$e_{\text{PDD}} := \frac{1}{L}\sum_{l=1}^{L}\left[R_i(\mathbf{x}^{(l)}) - \sum_{k=1}^{L_{S,m}} C_{i,k}\Psi_k(\mathbf{x}^{(l)})\right]^2, \tag{35}$$

committed by PDD. Denote by

$$\bar{\mathbf{A}} := \begin{bmatrix} \Psi_1(\mathbf{x}^{(1)}) & \cdots & \Psi_{L_{S,m}}(\mathbf{x}^{(1)}) \\ \vdots & \ddots & \vdots \\ \Psi_1(\mathbf{x}^{(L)}) & \cdots & \Psi_{L_{S,m}}(\mathbf{x}^{(L)}) \end{bmatrix} \tag{36}$$

and

$$\bar{\mathbf{b}} := \left\{R_i(\mathbf{x}^{(1)}),\dots,R_i(\mathbf{x}^{(L)})\right\}^{\intercal} \tag{37}$$

an $L\times L_{S,m}$ matrix and an L-dimensional column vector comprising evaluations of the orthonormal polynomial basis functions and output function at the data points, respectively. Then, the estimated coefficients $\tilde{C}_{i,j}$, $j=1,\dots,L_{S,m}$, are obtained as

$$\tilde{\mathbf{C}}_i := \left\{\tilde{C}_{i,1},\dots,\tilde{C}_{i,L_{S,m}}\right\}^{\intercal} = \left(\bar{\mathbf{A}}^{\intercal}\bar{\mathbf{A}}\right)^{-1}\bar{\mathbf{A}}^{\intercal}\bar{\mathbf{b}}. \tag{38}$$

Here, $\bar{\mathbf{A}}^{\intercal}\bar{\mathbf{A}}$ is an $L_{S,m}\times L_{S,m}$ matrix, often referred to as the information or data matrix. A necessary condition for the SLS solution is $L > L_{S,m}$, that is, the data size must be larger than the number of coefficients. Even when this condition is satisfied, the experimental design must be judiciously selected in such a way that the information matrix is well-conditioned.

5. Integrated PDD-NARX

The combination of Eqs. (16) and (33), with $R_i(\mathbf{X})$ replaced by $R_{i,S,m}(\mathbf{X})$, results in the desired PDD-NARX approximation:

$$\tilde{y}_{S',m';S,m}(t_j;\mathbf{X}) = \sum_{i=1}^{L'_{S',m'}}\left[\left\{\sum_{k=1}^{L_{S,m}} C_{i,k}\Psi_k(\mathbf{X})\right\}\Phi_i(\mathbf{z}(t_j;\mathbf{X}))\right]. \tag{39}$$

There are $L'_{S',m'}\times L_{S,m}$ terms in the approximation, depending on the expansion parameters of the NARX model function (S',m') and PDD (S,m) of NARX coefficients. These expansion parameters, including other parameters not symbolized explicitly, should be selected in such a way that the probabilistic characteristics of a time-dependent response of interest are calculated both accurately and efficiently. As the NARX and PDD approximations are individually mean-square convergent, the PDD-NARX approximation proposed should also provide mean-square convergent solutions.

Similar to existing PCE-NARX [18], the proposed PDD-NARX approximation in Eq. (39) can also be viewed as a surrogate of the exact map $y:[t_0,t_J]\times\mathbb{A}^N\to\mathbb{R}$. But there is one big advantage of PDD-NARX over PCE-NARX: the number of basis functions of PDD ($L_{S,m}$) grows with N much more slowly than that of PCE (L_m, say) if $S\ll N$, raising the potential for solving high-dimensional time-dependent UQ problems. More specifically, $L_{S,m}=\mathcal{O}(N^S)$ for large N, that is, the computational effort by an S-variate PDD approximation scales S-degree-polynomially with respect to N. For instance, if $S=1$ or 2, as it is anticipated to hold in applications, only linear or quadratic complexity is expected. In contrast, the number of basis functions of PCE for large N becomes $L_m=\mathcal{O}(N^m/m!)$, demanding exponential growth in order m and hence succumbing to the curse of dimensionality. If $S\ll m$, then PDD-NARX deflates the curse of dimensionality to a substantial extent.

5.1. Practical PDD-NARX

As the PDD coefficients $C_{i,k}$ mandate conducting N-dimensional integrations for their evaluations, they cannot be determined exactly when N is large or the PDF of $\mathbf{X}$ is a general function. In this work, an SLS regression is put forward for estimating the coefficients, albeit more advanced statistical techniques can be used as well [27,28]. Moreover, due to temporal discretization, the NARX coefficients $R_i(\mathbf{X})$ are also obtained approximately. In other words, given the values of expansion parameters S',m',S,m and other input parameters, one has to work with approximate PDD coefficients $\tilde{C}_{i,k}$ (say). Therefore, instead of Eq. (39), an actual, implementable PDD-NARX approximation of $y(t_j;\mathbf{X})$

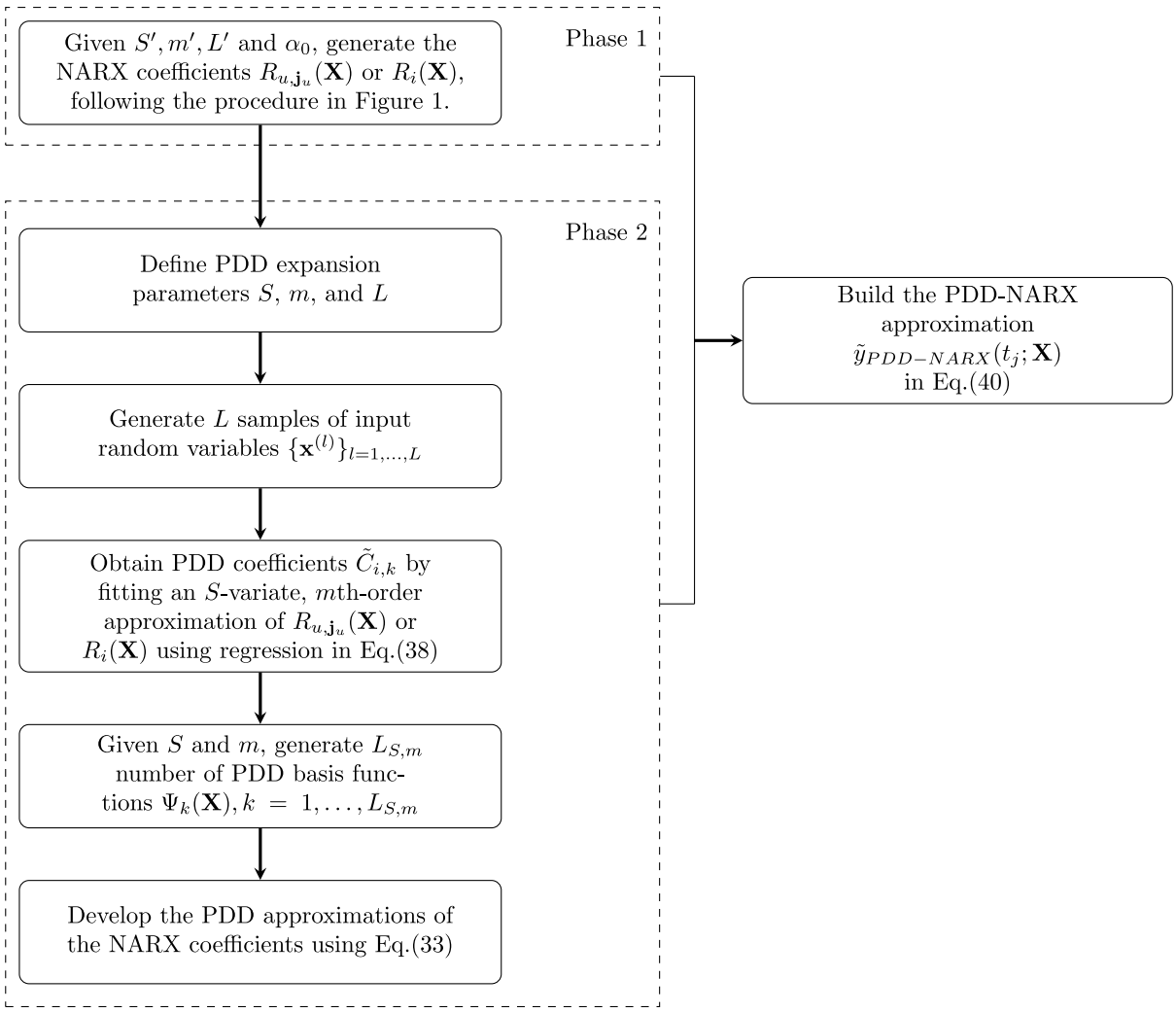

Fig. 2. A flow chart for constructing the PDD-NARX approximation for time-dependent UQ analysis.

is[6]

$$\tilde{y}_{\text{PDD-NARX}}(t_j;\mathbf{X}) = \sum_{i=1}^{L'_{S',m'}} \left[\left\{ \sum_{k=1}^{L_{S,m}} \tilde{C}_{i,k} \Psi_k(\mathbf{X}) \right\} \Phi_i(\mathbf{z}(t_j;\mathbf{X})) \right], \tag{40}$$

where the parametric symbols S', m', S, m determining $\tilde{y}_{\text{PDD-NARX}}(t_j;\mathbf{X})$ have been dropped for conciseness. Fig. 2 presents a computational flow for generating the actual PDD-NARX approximation for solving a general time-dependent UQ problem in two phases. Combining these two phases, each developed in conjunction with NARX and PDD approximations, leads to the desired PDD-NARX method. All numerical results, to be presented in forthcoming sections, are based on Eq. (40) for the PDD-NARX method.

5.2. Output statistics and probability distribution

Once the deterministic coefficients $\tilde{C}_{i,k}$, $i = 1,\ldots,L'_{S',m'}$, $k = 1,\ldots,L_{S,m}$, have been calculated, the PDD-NARX approximation in Eq. (40) furnishes an explicit function form in terms of elementary basis functions of NARX and PDD. Therefore, the statistical moments, such as the mean, variance, and higher-order moments, if they exist, can be easily estimated from MCS of the PDD-NARX approximation. For instance, the mean and variance estimates from the PDD-NARX approximation at time t_j are

$$\tilde{\mu}_{\text{PDD-NARX}}(t_j) = \frac{1}{L_{\text{MCS}}} \sum_{l=1}^{L_{\text{MCS}}} \tilde{y}_{\text{PDD-NARX}}(t_j;\mathbf{x}^{(l)}) \tag{41}$$

and

$$\tilde{\sigma}^2_{\text{PDD-NARX}}(t_j) = \frac{1}{L_{\text{MCS}}-1} \sum_{l=1}^{L_{\text{MCS}}} \left[\tilde{y}_{\text{PDD-NARX}}(t_j;\mathbf{x}^{(l)}) - \tilde{\mu}_{\text{PDD-NARX}}(t_j)\right]^2, \tag{42}$$

respectively, obtained using MCS with a sample size of $L_{\text{MCS}} \in \mathbb{N}$. Such simulation should not be confused with crude MCS, commonly used for producing benchmark results when possible. For complex problems, the crude MCS, which requires repeated calculations of $y(t_j;\mathbf{x}^{(l)})$ for input samples $\mathbf{x}^{(l)}$, $l = 1,\ldots,L_{MCS}$, can be highly expensive or even prohibitive when L_{MCS} needs to be very large for estimating small probabilities. In contrast, the MCS embedded in the PDD-NARX approximation requires evaluations of simple polynomial functions that describe $\tilde{y}_{\text{PDD-NARX}}(t_j;\mathbf{X})$. Therefore, a relatively large sample size can be accommodated in the PDD-NARX approximation even when $y(t_j;\mathbf{x}^{(l)})$ is expensive to calculate.

[6] If the PDF of $\mathbf{X}$ is arbitrarily prescribed, then an additional layer of approximation is also introduced in calculating numerically the measure-consistent non-classical orthogonal polynomials. However, it is not explicitly stated in Eq. (40).

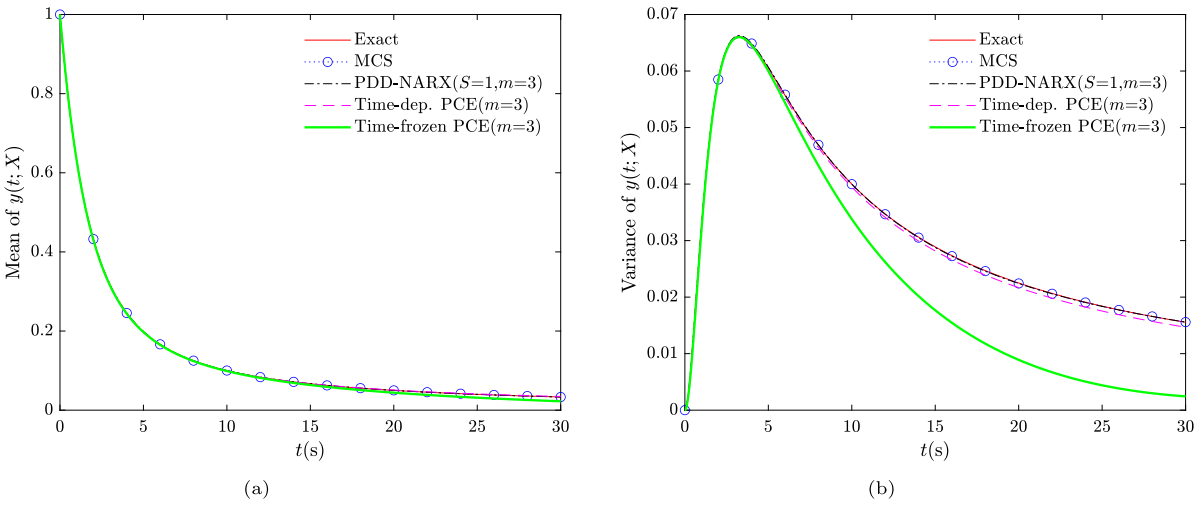

Fig. 3. Second-moment statistics of $y(t;X)$ and its approximations by five distinct methods; (a) mean; (b) variance.

Since PDD produces mean-square convergent solutions [8], the probability distribution function and density function of $y(t_j;\mathbf{X})$, if it exists, can also be estimated by MCS of the PDD-NARX approximation. Again, with the expansion coefficients of $\tilde{y}_{\text{PDD-NARX}}(t_j;\mathbf{X})$ calculated, the simulation can be performed inexpensively.

6. Numerical examples

Two numerical examples are presented to demonstrate the accuracy and efficiency of the proposed PDD-NARX method in calculating the statistical properties of various time-dependent system responses. The first example involves a simple, nonlinear stochastic ODE with a single random variable, serving as a fundamental test case for a rigorous comparison with existing UQ methods, including the time-frozen PCE and time-dependent PCE methods. In this context, the time-frozen PCE/PDD refers to the standard PCE/PDD approach that utilizes the same orthogonal polynomials to calculate the statistical properties of the response at any time $0 \le t \le T$. The second example illustrates PDD-NARX in handling a slightly more complex nonlinear problem from structural dynamics, involving a 2DOF quarter-car model with seven random variables.

In both examples, a crude MCS with a sample size of $L_{MCS} = 10^4$ was employed as the benchmark solution, ensuring an accurate reference for evaluating the precision and computational advantages of the PDD-NARX method. Table 1 lists the additional parameters of the NARX and PDD models or approximations used to generate the PDD-NARX solutions in this study. The samples of $y(t;\mathbf{X})$ required for estimating the NARX basis functions and PDD expansion coefficients via regression analysis were obtained from the exact solution in Example 1, and from a fourth-order Runge–Kutta numerical solution in Example 2.

6.1. Example 1: Stochastic ODE ($N = 1$)

In the first example, consider a stochastic initial-value problem described by the ODE

$$\frac{dy(t;X)}{dt} + Xy(t;X) = 0, \quad y(0;X) = 1, \tag{43}$$

where X is a single random variable ($N = 1$) uniformly distributed in the interval $[0,1]$ and $y(t;X)$ is the solution that depends on both time t and random variable X. A straightforward integration yields the exact solution: $y(t;X) = \exp(-Xt)$. Henceforth, the mean and variance of $y(t;X)$ can be exactly determined as

$$\mathbb{E}[y(t;X)] = \frac{1-\exp(-t)}{t} \tag{44}$$

Table 1
Input parameters for the NARX and PDD approximations used in examples and application.

Parameter	Example 1	Example 2	Application
t_0, s	0	0	2.7
T, s	30	30	4.9
Δt, s	0.01	0.01	–[a]
n_g	4	4	4
n_y	4	4	4
S'	2	2	2
m'	2	2	2
α_0	$0.1, 10^{-5}$	0.1	10^{-8}
S	1	1	1
m	3	3	3
L'	500	100	100
L	20	110	86, 128
L_{MCS}	10,000	10,000	300

[a] Varies from 0.01 and 0.02, as determined by ABAQUS.
Note: t_0 = initial time; T = final time; Δt = time step;
n_g, n_y = factors of time lags for excitation and response;
S', m' = interaction degree and order for NARX approx.;
α_0 = threshold of importance factor;
S, m = interaction degree and order for PDD approx.;
L', L, L_{MCS} = sample sizes for NARX, PDD, and MCS.

and

$$\mathbb{E}\left[(y(t;X) - \mathbb{E}[y(t;X)])^2\right] = \frac{1-\exp(-2t)}{2t} - \left(\frac{1-\exp(-t)}{t}\right)^2, \tag{45}$$

respectively.

The PDD-NARX approximation and a few other existing UQ methods were applied to estimate the mean and variance of $y(t;X)$. The NARX and PDD parameters employed in this example are listed in Table 1. For constructing the NARX model function, two distinct values of the threshold parameter $\alpha_0 = 0.1$ or 10^{-5} were selected, resulting in the final reduced number of NARX basis functions $L'_{S',m'} = 2$ and $L'_{S',m'} = 6$, respectively. Table 2 enumerates these basis functions for both values of the threshold parameter. For the PDD approximation of NARX coefficients, Legendre orthonormal polynomials, which are consistent with the uniform probability measure of X, were employed. For $S = N = 1, m = 3$, there are $L_{1,3} = 4$ basis functions of PDD.

Fig. 3(a) and Fig. 3(b) present the time histories of the mean and variance, respectively, of $y(t;X)$ and its approximation by five distinct methods or solutions: (1) exact solution, (2) crude MCS ($L_{MCS} = 10^4$), (3) univariate, third-order ($S = 1, m = 3$) PDD-NARX, (4) third-order

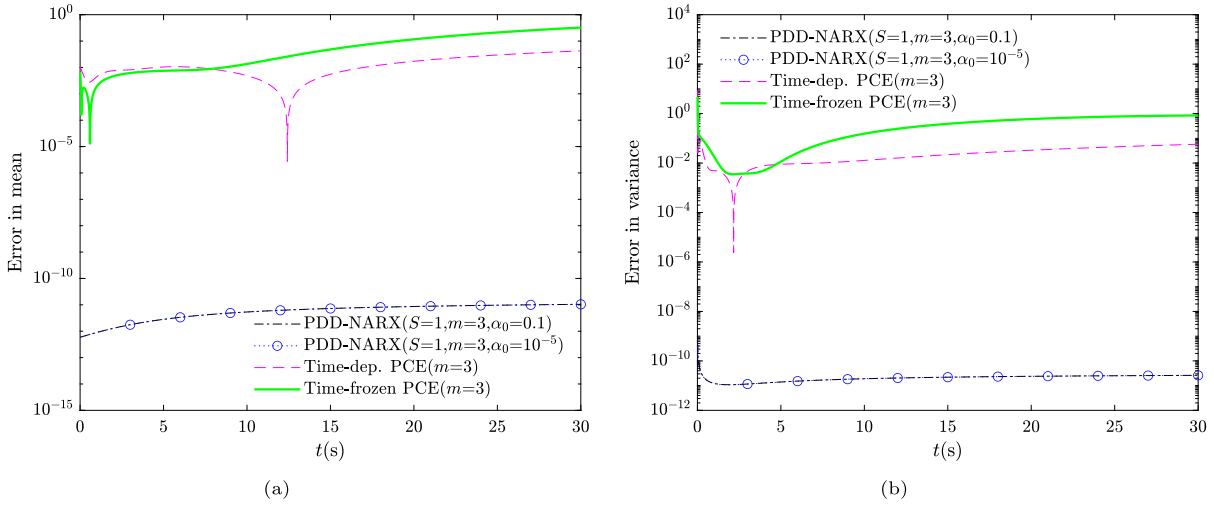

Fig. 4. Errors committed by third-order PDD-NARX, time-frozen PCE, and time-dependent PCE with respect to time; (a) mean; (b) variance.

Table 2
Basis functions of NARX in the stochastic ODE.

α_0	i	Basis function $[\Phi_i(\mathbf{z}(t_j;\mathbf{X}))]$
0.1	1	1
	2	$y(t_j-\Delta t;X)$
10^{-5}	1	1
	2	$y(t_j-\Delta t;X)$
	3	$y^2(t_j-\Delta t;X)$
	4	$y(t_j-2\Delta t;X)$
	5	$y(t_j-3\Delta t;X)$
	6	$y(t_j-4\Delta t;X)$

($m = 3$) time-frozen PCE [13], and (5) third-order ($m = 3$) time-dependent PCE [13]. The third-order approximations were selected, as the results of existing PCE whether time-dependent or time-frozen were readily available [13]. In these figures, the exact solutions of both moments and those obtained by MCS are virtually indistinguishable. Moreover, the mean of $y(t;X)$ for any time $0 \le t \le 30$ s in Fig. 3(a) by PDD-NARX and both variants of PCE are nearly identical to those calculated exactly or by MCS. However, the variance of $y(t;X)$ in Fig. 3(b) tells a different tale. Here, the time-frozen PCE is quite good until around $t = 7$ s, but the solution deteriorates soon thereafter and becomes exceedingly erroneous as time progresses. The time-dependent PCE, owing to incremental updates of orthogonal polynomials, markedly improves the approximation quality of time-frozen PCE, as expected. In contrast, the PDD-NARX method also provides excellent estimates of the variances at all time instants. Any difference between the PDD-NARX approximation and the exact or MCS solution is impalpable to the naked eye.

For a more quantitative assessment of the approximation quality of the PDD-NARX and existing PCE methods, Fig. 4(a) and Fig. 4(b) depict the errors in calculating the mean and variance of $y(t;X)$, respectively, committed by all three third-order ($m = 3$) UQ methods as a function of time. Here, the error is defined as the absolute value of the ratio of (1) the difference between the MCS solution and the approximate solution of interest and (2) the MCS solution. The results from both figures indicate that PDD-NARX commits errors substantially lower than those perpetrated by either version of PCE. For the PDD-NARX method, there are no notable changes in its approximation quality when the threshold parameter (α_0) is dropped from 0.1 to 10^{-5}. This suggests that only two basis functions obtained using $\alpha_0 = 0.1$, as listed in Table 2, are adequate for describing the NARX model function.

In addition, Fig. 5(a) and Fig. 5(b) display the errors in the mean and variance of $y(t;X)$, respectively, at a long time $t = 30$ s, achieved by all three aforementioned methods when the order of approximation (m) is steadily elevated. While the errors from all three methods decay expectedly with increasing orders, the PDD-NARX outperforms both variants of PCE by committing substantially lower error for any m.

6.2. Example 2: Stochastic dynamics of a 2DOF car model ($N = 7$)

The second example, studied by Mai et al. [18], involves conducting a nonlinear dynamic analysis of a quarter-car model subject to uncertainty. Comparing the results and performance of PDD-NARX with those generated by PCE-NARX is the principal motivation for solving this problem.

Fig. 6 provides a schematic representation of a 2DOF, quarter-car model, where m_s and m_u are the random sprung and unsprung masses, respectively, k_s and k_u are the random spring stiffnesses, respectively, and c is the random damping coefficient, characterizing the energy dissipation within the system. The car is subjected to a random road profile excitation $g(t;X) = A\sin(\omega t)$, where A and ω are the random amplitude and random frequency parameters. The nonlinear equations of motion for this 2DOF car model are given by [18]

$$\begin{aligned} m_s\ddot{y}_1(t;\mathbf{X}) &= -k_s(y_1(t;\mathbf{X})-y_2(t;\mathbf{X}))^3 - c(\dot{y}_1(t;\mathbf{X})-\dot{y}_2(t;\mathbf{X})),\\ m_u\ddot{y}_2(t;\mathbf{X}) &= k_s(y_1(t;\mathbf{X})-y_2(t;\mathbf{X}))^3 + c(\dot{y}_1(t;\mathbf{X})-\dot{y}_2(t;\mathbf{X})) + \\ &\quad k_u(g(t;\mathbf{X})-y_2(t;\mathbf{X})), \end{aligned} \tag{46}$$

where $y_1(t;\mathbf{X})$ and $y_2(t;\mathbf{X})$ are the displacements of sprung and unsprung masses, respectively.

In this example, both the system properties and excitation are uncertain. More specifically, the input random vector $\mathbf{X} = \{m_s, m_u, k_s, k_u, c, A, \omega\}^\intercal$ comprises seven input random variables ($N = 7$). Their means, standard deviations, and probability distributions are described in Table 3. All input random variables are mutually statistically independent.

The NARX and PDD parameters used in this example are also listed in Table 1. Here, the threshold parameter $\alpha_0 = 0.1$, resulting in the final, reduced number of NARX basis functions to be $L'_{S',m'} = 4$. The basis functions are as follows: 1, $y_1(t_j-\Delta t;\mathbf{X})$, $y_1(t_j-2\Delta t;\mathbf{X})$, and $y_1(t_j-3\Delta t;\mathbf{X})$. For the PDD approximation of NARX coefficients, Hermite and Legendre orthonormal polynomials, which are consistent with the Gaussian and uniform probability measures of input random variables, were employed. For $S = 1, m = 3$, there are $L_{1,3} = 22$ basis functions of PDD. As there is no exact solution in this example, the reference solution used to judge the approximation quality of PDD-NARX is crude MCS with the sample size $L_{MCS} = 10^4$.

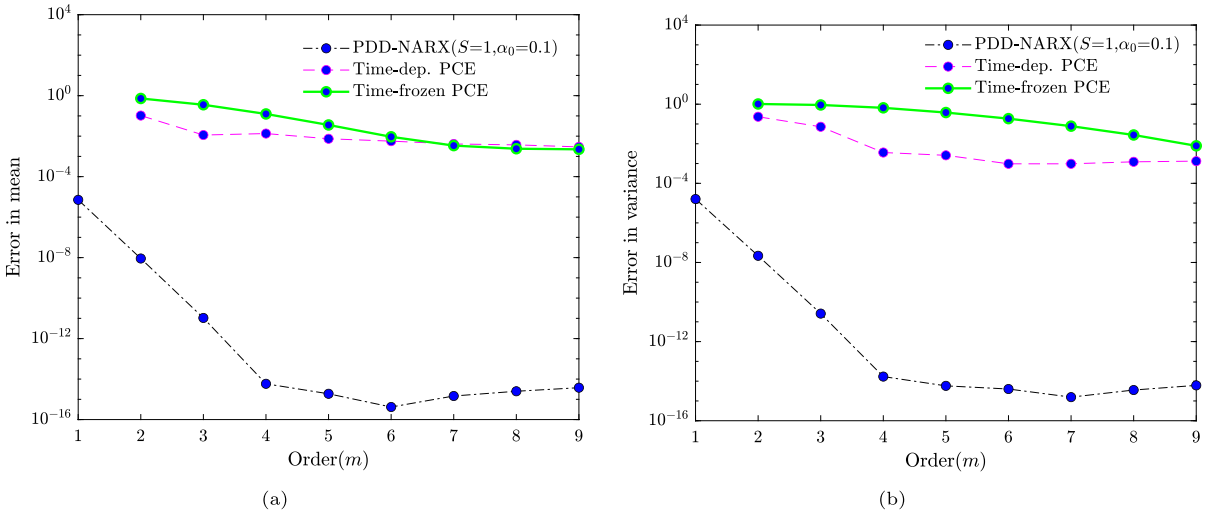

Fig. 5. Errors committed by PDD-NARX, time-frozen PCE, and time-dependent PCE at $t = 30$ s with respect to orders of approximation; (a) mean; (b) variance.

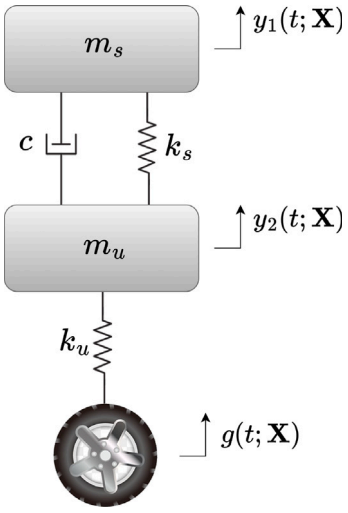

Fig. 6. A 2DOF model of a quarter-car.

Table 3
Statistical properties of the input random variables in the 2DOF car model.

Random variable	Probability distribution	Mean	Standard deviation
m_s, kg	Gaussian	20	2
m_u, kg	Gaussian	40	4
k_s, N/m	Gaussian	2000	200
k_u, N/m	Gaussian	2000	200
c, N-s/m	Gaussian	600	60
A, m	Uniform	0.1	$\frac{(0.11-0.9)}{\sqrt{12}}$
ω, rad/s	Uniform	2π	$\frac{(2.2\pi-1.8\pi)}{\sqrt{12}}$

Note: m_s, m_u = sprung and unsprung masses, resp.; k_s, k_u = spring stiffnesses c, A, ω = damping coefficient, excitation amplitude, excitation frequency, respectively.

Due to the input uncertainty, any dynamic response of the car model is stochastic. For brevity, only the probabilistic characteristics of the sprung mass displacement, that is, $y_1(t;\mathbf{X})$, was studied. Fig. 7(a) and Fig. 7(b) delineate the mean and standard deviation of $y_1(t;\mathbf{X})$ for $0 \le t \le 30$ s, estimated by the univariate, third-order PDD-NARX and third-order PCE-NARX approximations. For both approximations, the corresponding results of their time-frozen versions are also included. According to Fig. 7(a), the means of $y_1(t;\mathbf{X})$ by all methods including crude MCS show similar trends or values, albeit the time-frozen PCE or time-frozen PDD exhibits greater oscillations when t is large. In Fig. 7(b), the time-frozen versions struggle to accurately predict the standard deviation from MCS, especially when $t \ge 4$ s. In contrast, the PDD-NARX and PCE-NARX methods both demonstrate strong agreement with the benchmark solution of MCS, verifying the accuracy of the former methods in estimating these two moments at all time instants.

While the results of PDD-NARX and PCE-NARX appear practically identical in accuracy, their relative computational efforts differ significantly. In this particular example, PCE-NARX requires 600 sample data to achieve the reported accuracy, whereas PDD-NARX attains the same level of precision with only 110 sample data (L). This is possible as the third-order PDD utilizes only $L_{1,3} = 22$ univariate basis functions, which are more than adequate for constructing the PDD-NARX approximation without sacrificing the solution accuracy. In contrast, the third-order PCE employs 120 basis functions, entailing not only univariate, but also unneeded or unimportant higher-variate basis functions, thus incurring additional cost for estimating the associated expansion coefficients.

Beyond the second-moment analysis, a comparison between the probability distributions of the dynamic responses generated using PDD-NARX and PCE-NARX should be intriguing. In this regard, Fig. 8(a), Fig. 8(b), and Fig. 8(c) illustrate the PDFs of (1) the sprung displacement $y_1(5;\mathbf{X})$ at time $t = 5$ s; (2) the sprung displacement $y_1(30;\mathbf{X})$ at time $t = 30$ s; and (3) maximum absolute sprung displacement $\max_{0\le t\le 30} |y_1(t;\mathbf{X})|$, respectively. As observed from the analysis of statistical moments, both methods also produce PDFs matching the MCS results extremely well, but PDD-NARX is still more computationally efficient than PCE-NARX by a factor of nearly six. The substantial reduction in computational cost underscores the efficiency of PDD-NARX, making it a highly effective approach for UQ analysis of complex dynamical systems, to be demonstrated next.

7. Application

This section highlights the practical application of the PDD-NARX method in tackling a complex vehicle-dynamics problem involving 21 random variables. The focus of the application is dynamic analysis of a Chevrolet C1500 pick-up truck riding over anti-symmetric road bumps, as depicted in Fig. 9(a). The analysis illustrates the capability of the PDD-NARX method to efficiently handle high-dimensional UQ in a real-world engineering scenario, showcasing its potential for addressing complex, large-scale problems.

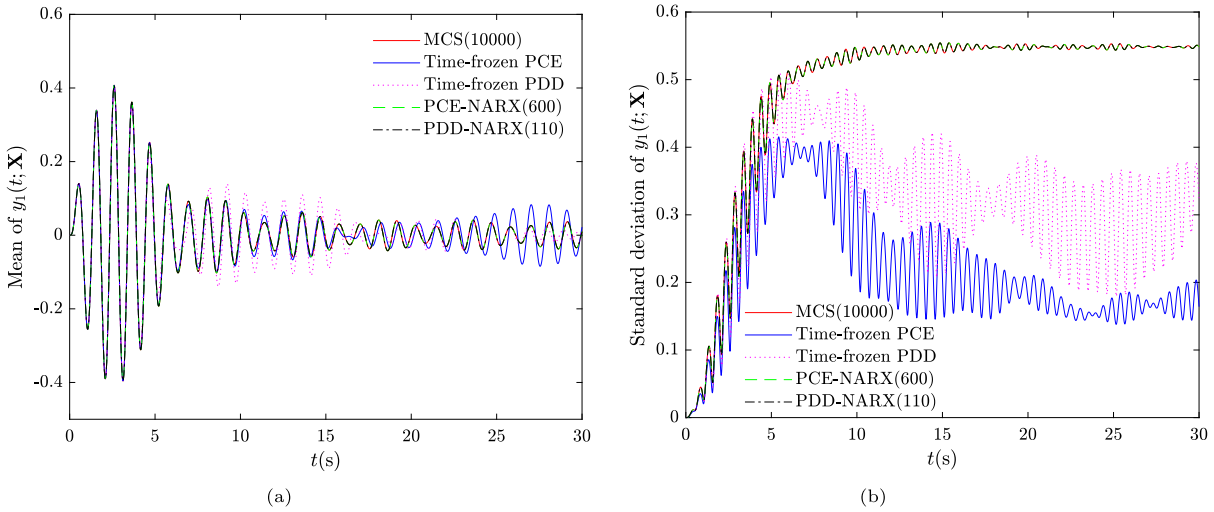

Fig. 7. Second-moment statistics of $y_1(t;\mathbf{X})$ calculated by various methods for the car model; (a) mean; (b) standard deviation.

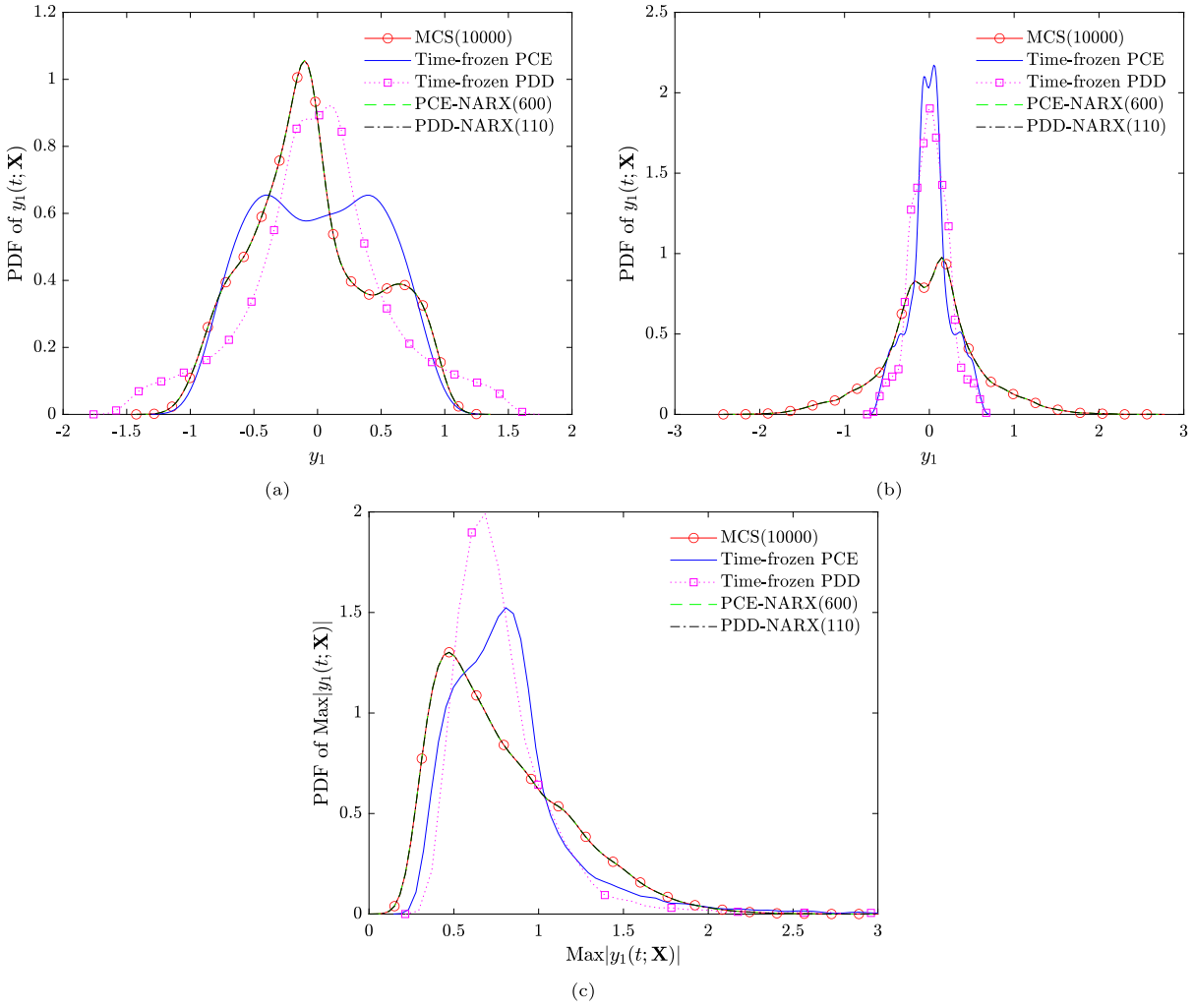

Fig. 8. Probability density functions of the sprung mass displacement of the car model calculated by various methods; (a) $y_1(5;\mathbf{X})$; (b) $y_1(30;\mathbf{X})$; (c) $\max_{0\le t\le 30}|y_1(t;\mathbf{X})|$.

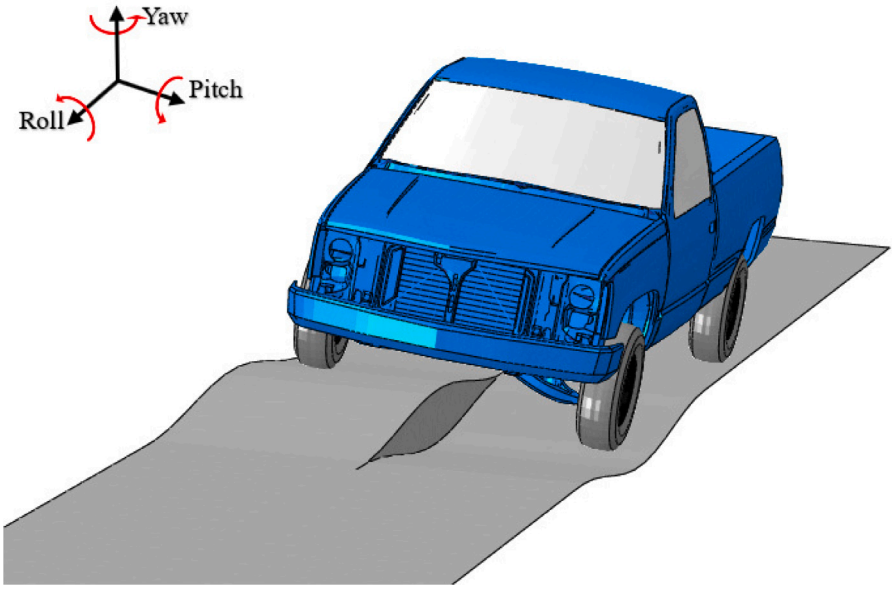

(a)

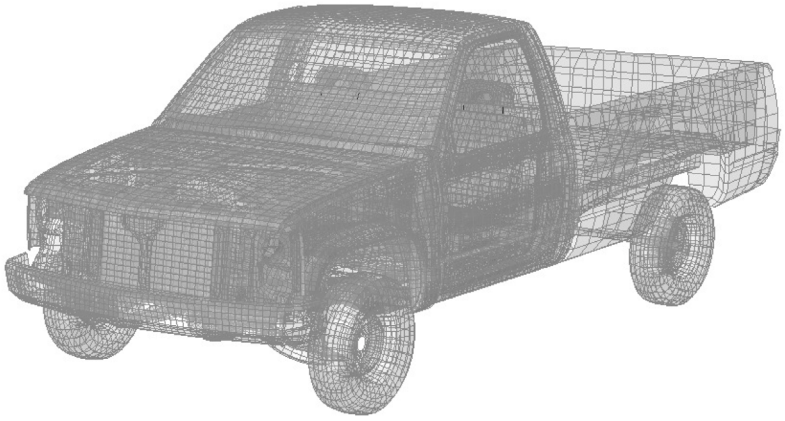

(b)

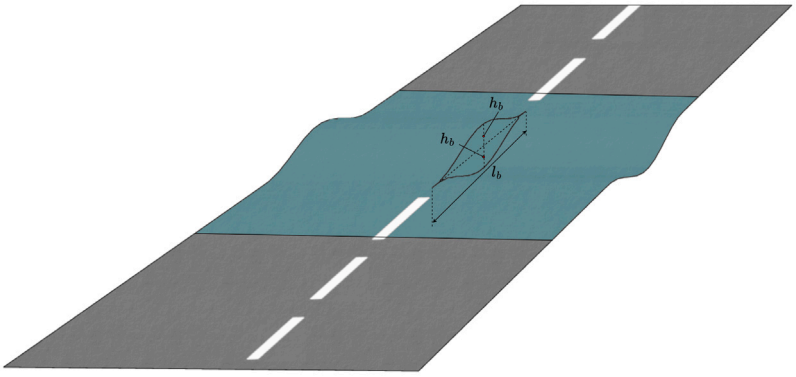

(c)

Fig. 9. A Chevrolet pick-up truck; (a) truck riding over anti-symmetric bumps; (b) FEA discretization with nearly 55,000 elements; (c) anti-symmetric road bumps.

7.1. Finite element analysis

A well-known commercial code for finite element analysis (FEA), named ABAQUS (Version 2024) [29], was utilized to discretize the truck geometry using approximately 55,000 elements. The FEA model, displayed in Fig. 9(b), consists of various parts, such as the cabin, truck bed, doors, and other components, which are meshed with shell elements, three-dimensional beam elements, and three-dimensional solid elements. The parts are connected using connector elements, coupling elements, and multi-point constraints. Additional details of FEA modeling and simulation are available in "Section 3.2.2 Substructure Analysis of a Pick-up Truck Model" of the ABAQUS Example manual [29].

The dynamic analysis involves the pick-up truck driving over anti-symmetric road bumps. The bumps consist of two random geometric parameters: bump height h_b and bump length l_b, as sketched schematically in Fig. 9(c). The height of the bump varies spatially according to a nearly Gaussian distribution along its length. The system includes two such bumps in an anti-symmetric arrangement, where one of the bumps is inverted, as displayed in Fig. 9(c). For dynamic analysis, only anti-symmetric road bumps were considered in this work. This configuration is commonly used to evaluate the vehicle's response to the applied forces from the road bumps in the automotive industry.

The substructure capability of ABAQUS was employed to efficiently simulate the vehicle-dynamics of the truck model as it traverses over road bumps. The truck was loaded statically by gravity first, and then accelerated (5 m/s^2) to the desired velocity of 8 m/s on a flat road. Once the cruise velocity was achieved, the truck model was run over anti-symmetric bumps.

7.2. Material properties

The materials used in the FEA truck model include steel, plastic, glass, rubber, rubber–metal composite, and foam for representing a wide variety of parts. Their mechanical behavior is either elastic or elastic–plastic. A detailed description of these materials and their properties is too extensive to be included here, but they can be found in Tables 3.2.1–1 and 3.2.1–2 of the ABAQUS Example manual available in the open literature [29].

Fig. 10 provides a color-coded breakdown of the six major different material types utilized in the truck model. Types 1, 2, 4, and 6 are made of steel, while Types 3 and 5 are made of plastic and rubber, respectively. For the kth material type ($k = 1, \ldots, 6$), the Young's modulus, Poisson's ratio, and mass density are denoted by E_k, ν_k, and ρ_k, respectively. Additionally, the radial stiffness of the tire is represented by K_R. In total, 19 material parameters were identified as random input in this application. These input material properties are critical for accurately simulating the truck's dynamic behavior and analyzing the response to the road bump interactions.

7.3. Input random variables

The input comprises 21 random variables describing two random geometric parameters of the road bumps and 19 random material properties of the truck and tire, described in the preceding sections. The random variables follow independent truncated Gaussian distributions. Their respective means, coefficients of variations, and bounds are provided in Table 4. For all material properties, including the tire's radial stiffness, the probability distribution is defined with a lower limit $a_i = 0.8\mu_i$, an upper limit $b_i = 1.2\mu_i$, where μ_i is the mean value of the variable from Table 4, and a 10 percent coefficient of variation. For the bump height and bump length, the probability distribution is characterized by a lower limit of $a_i = 0.7\mu_i$, an upper limit of $b_i = 1.3\mu_i$, and a 20 percent coefficient of variation. These constraints ensure that the random variables remain within physically meaningful bounds while capturing the inherent uncertainties in the system parameters.

Table 4
Mean, coefficient of variation, and bounds of 21 input random variables in the pick-up truck model.

i	Random variable	Mean (μ_i)	Coefficient of variation (%)	Bounds
1	E_1, MPa	210,000	10	$[0.8\mu_1, 1.2\mu_1]$
2	E_2, MPa	210,000	10	$[0.8\mu_2, 1.2\mu_2]$
3	E_3, MPa	3400	10	$[0.8\mu_3, 1.2\mu_3]$
4	E_4, MPa	210,000	10	$[0.8\mu_4, 1.2\mu_4]$
5	E_5, MPa	246,000	10	$[0.8\mu_5, 1.2\mu_5]$
6	E_6, MPa	210,000	10	$[0.8\mu_6, 1.2\mu_6]$
7	ν_1	0.3	10	$[0.8\mu_7, 1.2\mu_7]$
8	ν_2	0.3	10	$[0.8\mu_8, 1.2\mu_8]$
9	ν_3	0.3	10	$[0.8\mu_9, 1.2\mu_9]$
10	ν_4	0.3	10	$[0.8\mu_{10}, 1.2\mu_{10}]$
11	ν_5	0.323	10	$[0.8\mu_{11}, 1.2\mu_{11}]$
12	ν_6	0.3	10	$[0.8\mu_{12}, 1.2\mu_{12}]$
13	ρ_1, kg/m^3	7890	10	$[0.8\mu_{13}, 1.2\mu_{13}]$
14	ρ_2, kg/m^3	7890	10	$[0.8\mu_{14}, 1.2\mu_{14}]$
15	ρ_3, kg/m^3	1100	10	$[0.8\mu_{15}, 1.2\mu_{15}]$
16	ρ_4, kg/m^3	7890	10	$[0.8\mu_{16}, 1.2\mu_{16}]$
17	ρ_5, kg/m^3	8060	10	$[0.8\mu_{17}, 1.2\mu_{17}]$
18	ρ_6, kg/m^3	7890	10	$[0.8\mu_{18}, 1.2\mu_{18}]$
19	K_R, N/mm	600	10	$[0.8\mu_{19}, 1.2\mu_{19}]$
20	h_b, mm	200	20	$[0.7\mu_{20}, 1.3\mu_{20}]$
21	l_b, mm	5000	20	$[0.7\mu_{21}, 1.3\mu_{21}]$

Note: E_k = Young's modulus of kth material; ν_k = Poisson's ratio of kth material; ρ_k = mass density of kth material; K_R = radial stiffness of tire; h_b = bump height; l_b = bump length.

7.4. Results and discussion

The primary objective of this application is to compute the vehicle body motion angles or rotations, which serve as key indicators of the truck's dynamic behavior. There are three such angles or rotations: roll, pitch, and yaw, as schematically depicted in Fig. 9(a). Therefore, $y(t;\mathbf{X})$ in this work represents any one of these three motion angles at the vehicle's center of gravity (CG).

The NARX and PDD parameters used in this application are also defined in Table 1. All sample time histories of $y(t;\mathbf{X})$ were generated by direct numerical simulation from ABAQUS. Using a high-performance desktop personal computer, each run of the ABAQUS substructure analysis took approximately an hour of CPU time. Consequently, generating 300 time histories from ABAQUS simulations required more than 12 days of computational time. In this work, 86 or 128 samples of these time histories were used to build the PDD-NARX approximations. Due to the high computational expense of the large-scale simulation, only $L_{MCS} = 300$ samples were used to estimate the second-moment statistics by MCS.

7.4.1. Deterministic analysis

In order to evaluate the accuracy of constructing the NARX model function, the roll, pitch, and yaw at the truck's CG were investigated under a deterministic condition where all 21 input variables were assigned their mean values, as listed in Table 4. In this case, there is no variability in the system parameters, and the PDD-NARX method simplifies to a deterministic NARX model. For this deterministic input, two sets of the time histories of roll, pitch, and yaw were calculated using (1) the combined dimension-wise tensor product expansion and basis reduction procedure developed in this work; and (2) direct numerical simulation from the ABAQUS substructure analysis. A comparison between these two time histories in Fig. 11(a), Fig. 11(b), and Fig. 11(c), obtained separately for roll, pitch, and yaw, indicate excellent agreement between the two respective solutions. The high accuracy of the proposed dimension-wise tensor product expansion with basis reduction provides confidence on the fidelity of subsequent statistical analysis, to be presented next.

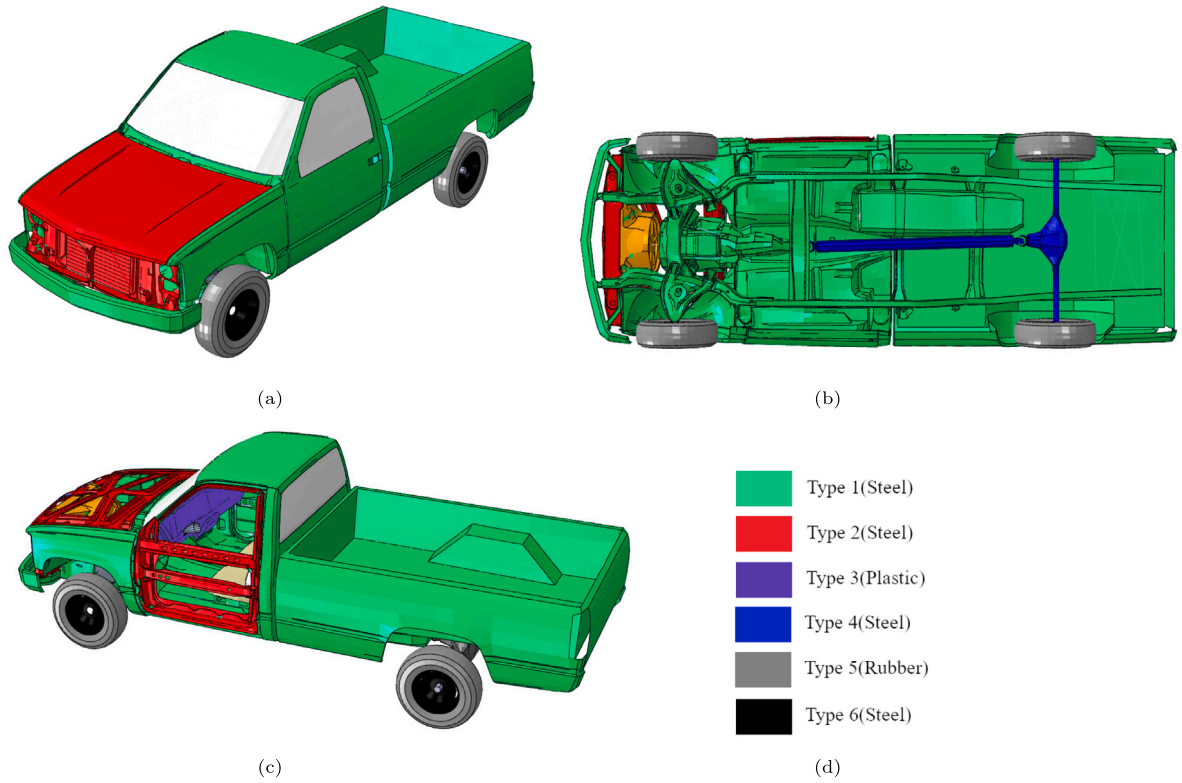

Fig. 10. Material distribution in the pick-up truck; (a) isometric view; (b) bottom view; (c) side and interior view; (d) color legends for six material types.

Table 5
Basis functions of NARX in the pick-up truck model.

α_0	i	Basis function $[\Phi_i(\mathbf{z}(t_j;\mathbf{X}))]$	Importance rank for roll[a]	Importance rank for pitch[a]
	1	1	15	15
	2	$y(t_j-\Delta t;\mathbf{X})$	11	12
	3	$y(t_j-2\Delta t;\mathbf{X})$	12	11
	4	$y(t_j-3\Delta t;\mathbf{X})$	14	13
	5	$y(t_j-4\Delta t;\mathbf{X})$	13	14
	6	$y^2(t_j-\Delta t;\mathbf{X})$	9	9
	7	$y^2(t_j-2\Delta t;\mathbf{X})$	5	3
10^{-8}	8	$y^2(t_j-3\Delta t;\mathbf{X})$	2	2
	9	$y^2(t_j-4\Delta t;\mathbf{X})$	10	10
	10	$y(t_j-\Delta t;\mathbf{X})y(t_j-2\Delta t;\mathbf{X})$	7	4
	11	$y(t_j-\Delta t;\mathbf{X})y(t_j-3\Delta t;\mathbf{X})$	6	7
	12	$y(t_j-\Delta t;\mathbf{X})y(t_j-4\Delta t;\mathbf{X})$	8	8
	13	$y(t_j-2\Delta t;\mathbf{X})y(t_j-3\Delta t;\mathbf{X})$	1	1
	14	$y(t_j-2\Delta t;\mathbf{X})y(t_j-4\Delta t;\mathbf{X})$	3	6
	15	$y(t_j-3\Delta t;\mathbf{X})y(t_j-4\Delta t;\mathbf{X})$	4	5

[a] Ranking index varies from 1 (highest) to 15 (lowest).

7.4.2. Statistical analysis

Due to uncertain bump geometry and material properties of the truck, a more realistic evaluation of roll and pitch requires calculating their statistical characteristics. To do so, the NARX model function has to be built first. Using 100 samples of $y(t;\mathbf{X})$, the NARX model function was constructed using the dimension-wise tensor product expansion and basis reduction with the chosen threshold parameter $\alpha_0 = 10^{-8}$. The second column of Table 5 lists 15 basis functions of NARX retained and used for subsequent probabilistic analysis by PDD-NARX. The third and fourth columns of Table 5 provide the rankings of these basis functions by comparing the importance factors for roll and pitch, respectively. It is interesting to note that the most important basis function of NARX stems from an interactive term (13th basis), which is not necessarily intuitive and hence cannot be ascertained *a priori*.

Given that the yaw angle is small and less oscillatory in this application, the statistical analysis was focused on roll and pitch angles only. Figs. 12 and 13 present the second-moment statistics, such as means and standard deviations, of roll and pitch at truck's CG as a function of time, obtained using two variants of the PDD-NARX: (1) a univariate, second-order ($S = 1, m = 2$) PDD-NARX approximation built from 86 samples of time histories; and (2) a univariate, third-order PDD-NARX ($S = 1, m = 3$) approximation constructed from 128 samples of time histories. The results of both variants of the PDD-NARX are practically coincident, meaning that the second-order approximation is sufficient, at least for this application. Comparing these PDD-NARX solutions and MCS-generated statistics in these two aforementioned figures, the agreement among them is excellent. Therefore, the PDD-NARX method – especially, the univariate, second-order approximation – developed in this work is capable of solving high-dimensional, complex engineering problems at the cost of less than a hundred numerical simulations.

8. Future work

While the paper provides a practical approach for conducting time-dependent UQ analysis, there are still a few open questions. First, the input random variables, assumed to be independently distributed in this work, should allow for correlated or dependent probability distributions in solving a broader class of problems. In which case, a generalized version of PDD, preferably employing measure-consistent multivariate orthogonal polynomials, will have to be developed.

Second, there is a need to establish an adaptive version of PDD-NARX, where a truncated set of basis is selected optimally based on a specified error tolerated by the resulting approximation. By doing so, the requirement for arbitrarily deciding on the degree of interaction and order of NARX or PDD approximation is avoided. These improvements are subjects of active research by the authors.

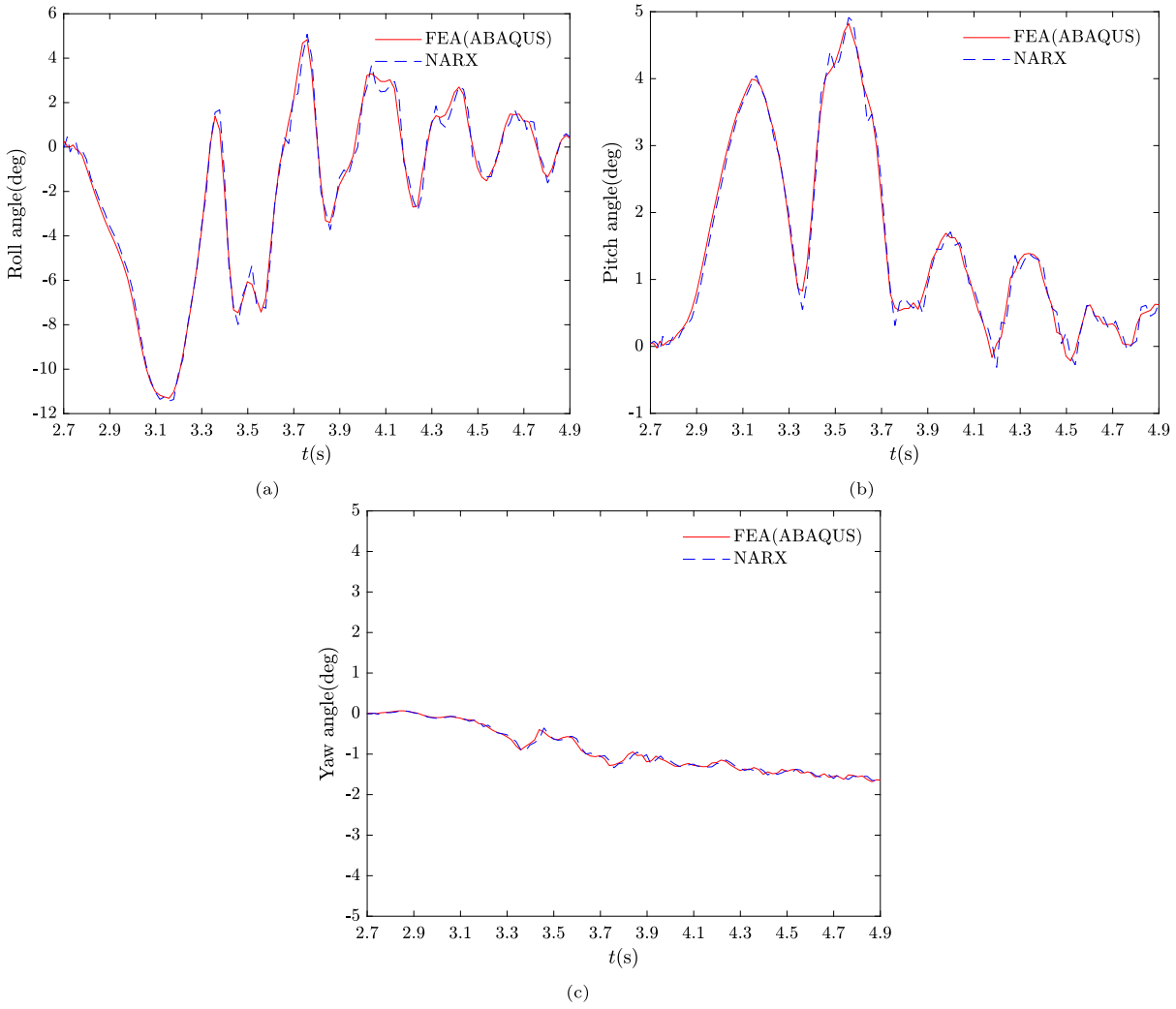

Fig. 11. Angular rotations at the truck's center of gravity for deterministic input parameters; (a) roll; (b) pitch; (c) yaw.

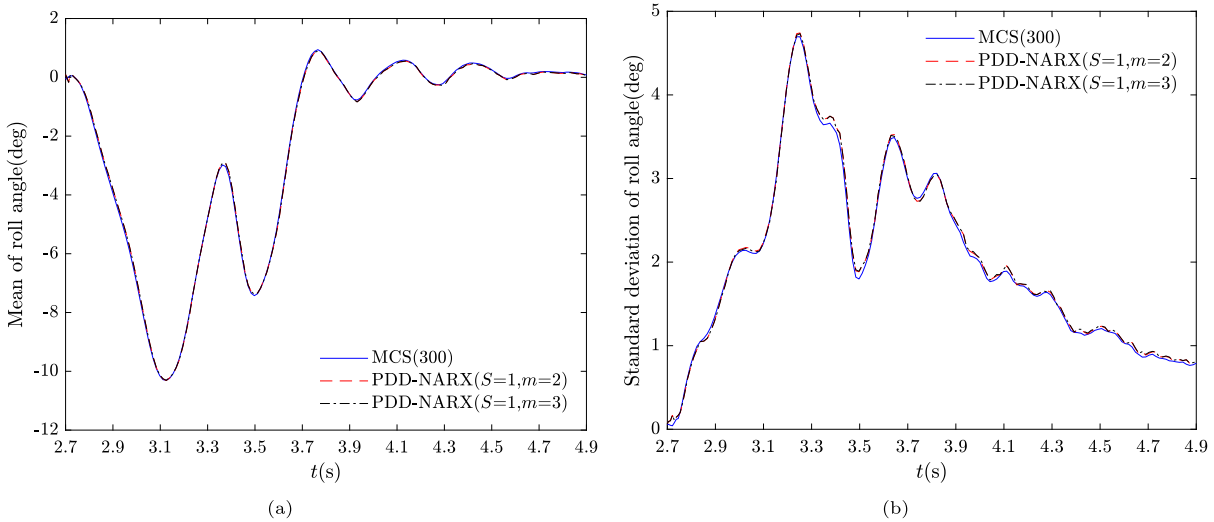

Fig. 12. Second-moment statistics of roll at truck's center of gravity; (a) mean; (b) standard deviation.

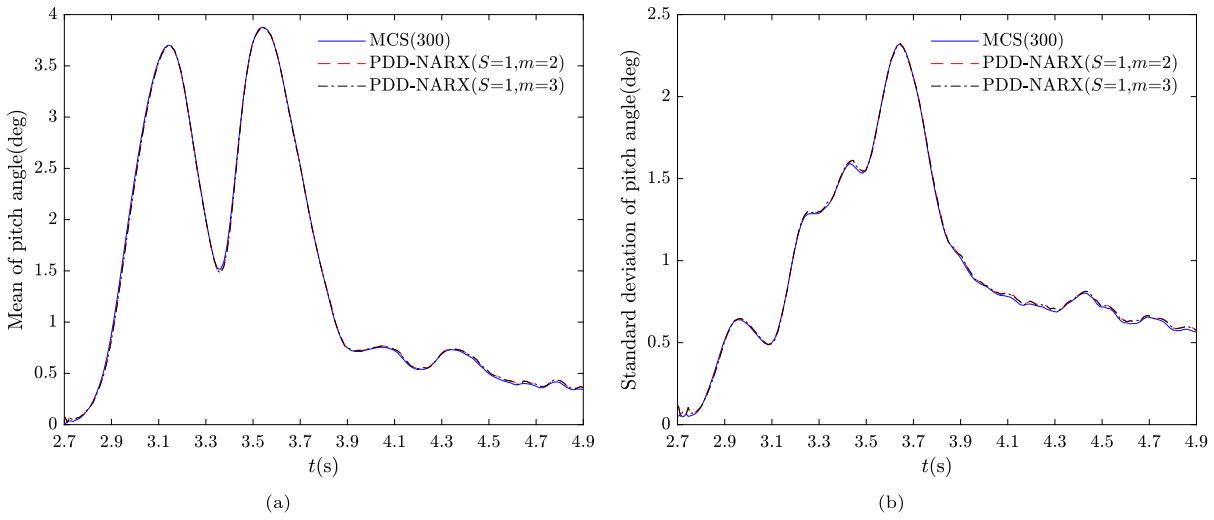

Fig. 13. Second-moment statistics of pitch at truck's center of gravity; (a) mean; (b) standard deviation.

9. Conclusion

A novel computational methodology, referred to as PDD-NARX, was developed for general time-dependent UQ analysis of complex dynamical systems. This method is applicable to both linear and nonlinear dynamical systems, and is distinguished by two key features that are attributed to the NARX and PDD components independently.

First, a dimension-wise tensor product expansion, coupled with a four-step algorithm for basis reduction, was established for the stochastic adaptation of the NARX model, enabling it to effectively capture the behavior of the dynamical system. Rather than relying on ad hoc or intuitive selection methods, the proposed approach offers an efficient, systematic strategy for identifying the necessary NARX basis functions. Second, the PDD approximation was exploited to retain low-dimensional interactions among input random variables, which is crucial for efficiently transmitting input uncertainty to the random NARX coefficients. This process effectively decelerates the growth in the number of PDD basis functions, which typically scale exponentially, by making their expansion scale polynomially instead. Specifically, if a univariate or bivariate PDD approximation is sufficient, the resulting computational complexity becomes linear or quadratic, mitigating the curse of dimensionality to a great extent. As a result, the PDD-NARX method is well-suited for solving high-dimensional, time-dependent UQ problems often encountered in industrial-scale applications.

Numerical results derived from the statistical moment analysis of a stochastic ODE demonstrate that the PDD-NARX approximation outperforms both time-frozen PCE and time-dependent PCE solutions in terms of approximation quality. Moreover, the time histories of the means and standard deviations of dynamic responses from a two-degree-of-freedom car model, including their probability distributions at discrete time instances, reveal that PDD-NARX achieves accuracy comparable to PCE-NARX while being significantly more computationally efficient — up to nearly six times faster. Lastly, the successful execution of a 21-dimensional UQ analysis for a 55,000-element pick-up truck further demonstrates the practicality and scalability of the PDD-NARX method for solving complex, large-scale engineering problems.

CRediT authorship contribution statement

M. Ebadollahi: Writing – review & editing, Visualization, Validation, Software, Methodology, Formal analysis, Data curation. **S. Rahman:** Writing – review & editing, Writing – original draft, Methodology, Investigation, Funding acquisition, Formal analysis, Data curation, Conceptualization.

Declaration of competing interest

The authors declare that they have no known competing financial interests or personal relationships that could have appeared to influence the work reported in this paper.

Data availability

Data will be made available on request.

References

[1] T.J. Sullivan, Introduction to Uncertainty Quantification, New York, Springer, 1971.
[2] R.C. Smith, Uncertainty Quantification, SIAM, 2013.
[3] M. Grigoriu, Stochastic Calculus: Applications in Science and Engineering, Birkhauser, 2002.
[4] N. Wiener, The homogeneous chaos, Amer. J. Math. 60 (4) (1938) 897–936.
[5] R.H. Cameron, W.T. Martin, The orthogonal development of non-linear functionals in series of Fourier–Hermite functionals, Ann. Math. 48 (1947) 385–392.
[6] R. Ghanem, P.D. Spanos, Stochastic Finite Elements: A Spectral Approach, World Publishing Corp., 1991.
[7] S. Rahman, A polynomial dimensional decomposition for stochastic computing, Internat. J. Numer. Methods Engrg. 76 (2008) 2091–2116.
[8] S. Rahman, Mathematical properties of polynomial dimensional decomposition, SIAM/ ASA J. Uncertain. Quantif. 6 (2018) 816–844.
[9] I. Babuska, F. Nobile, R. Tempone, A stochastic collocation method for elliptic partial differential equations with random input data, SIAM J. Numer. Anal. 45 (3) (2007) 1005–1034.
[10] B. Ganapathysubramanian, N. Zabaras, Sparse grid collocation schemes for stochastic natural convection problems, J. Comput. Phys. 225 (1) (2007) 652–685.
[11] S. Smolyak, Quadrature and interpolation formulas for tensor products of certain classes of functions, Dokl. Akad. Nauk SSSR 4 (1963) 240–243.
[12] T. Gerstner, M. Griebel, Numerical integration using sparse grids, Numer. Algorithms 18 (1998) 209–232.
[13] M. Gerritsma, J.B. Van der Steen, P. Vos, G. Karniadakis, Time-dependent generalized polynomial chaos, J. Comput. Phys. 229 (2010) 8333–8363.
[14] X. Wan, G. Karniadakis, Long-term behavior of polynomial chaos in stochastic flow simulations, Comput. Methods Appl. Mech. Engrg. 195 (2006) 5582–5596.
[15] V. Heuveline, M. Schick, A hybrid generalized polynomial chaos method for stochastic dynamical systems, Int. J. Uncertain. Quantif. 4 (2014) 37–61.
[16] S.A. Billings, Nonlinear System Identification: NARMAX Methods in the Time, Frequency, and Spatio-Temporal Domains, John Wiley & Sons, 2013.
[17] M.D. Spiridonakos, E.N. Chatzi, Metamodeling of dynamic nonlinear structural systems through polynomial chaos NARX models, Comput. Struct. 157 (2015) 99–113.
[18] C.V. Mai, M.D. Spiridonakos, E.N. Chatzi, B. Sudret, Surrogate modeling for stochastic dynamical systems by combining nonlinear autoregressive with exogenous input models and polynomial chaos expansions, Int. J. Uncertain. Quantif. 16 (2016) 313–339.

[19] W. Hoeffding, A class of statistics with asymptotically normal distribution, Ann. Math. Stat. 19 (3) (1948) 293–325.
[20] S. Rahman, Approximation errors in truncated dimensional decompositions, Math. Comp. 83 (290) (2014) 2799–2819.
[21] H. Rabitz, O. Alis, General foundations of high dimensional model representations, J. Math. Chem. 25 (1999) 197–233, 10.1023/A:1019188517934.
[22] B. Efron, C. Stein, The Jackknife estimate of variance, Ann. Statist. 9 (3) (1981) 586–596.
[23] W. Gautschi, Orthogonal Polynomials: Computation and Approximation, in: Numerical Mathematics and Scientific Computation, Oxford University Press, 2004.
[24] S. Rahman, Extended polynomial dimensional decomposition for arbitrary probability distributions, J. Eng. Mech. 135 (12) (2009) 1439–1451.
[25] V. Yadav, S. Rahman, Adaptive-sparse polynomial dimensional decomposition for high-dimensional stochastic computing, Comput. Methods Appl. Mech. Engrg. 274 (2014) 56–83.
[26] X. Ren, V. Yadav, S. Rahman, Reliability-based design optimization by adaptive-sparse polynomial dimensional decomposition, Struct. Multidiscip. Optim. 53 (3) (2016) 425–452.
[27] G. Li, H. Rabitz, D-MORPH regression: application to modeling with unknown parameters more than observation data, J. Math. Chem. 48 (2010) 1010–1035.
[28] B. Efron, T. Hastie, I. Johnstone, R. Tibshirani, Least angle regression, Ann. Stat. 32 (2004) 407–499.
[29] Abaqus Standard, Version 2024, Dassault Systems Simulia Corp., 2024.